

AN INVESTIGATION OF THE G2 CHECKPOINT

by

DARKO CURMAN

B.Sc., University of British Columbia, 1996

A THESIS SUBMITTED IN PARTIAL FULFILLMENT OF

THE REQUIREMENTS FOR THE DEGREE OF

Master of Science

in

THE FACULTY OF GRADUATE STUDIES

Department of Biochemistry and Molecular Biology

We accept this thesis as conforming

to the required standard

THE UNIVERSITY OF BRITISH COLUMBIA

December 1999

© Darko Curman, 1999

In presenting this thesis in partial fulfilment of the requirements for an advanced degree at the University of British Columbia, I agree that the Library shall make it freely available for reference and study. I further agree that permission for extensive copying of this thesis for scholarly purposes may be granted by the head of my department or by his or her representatives. It is understood that copying or publication of this thesis for financial gain shall not be allowed without my written permission.

Department of BIOCHEMISTRY AND MOLECULAR BIOLOGY

The University of British Columbia
Vancouver, Canada

Date DEC. 20 / 99

Abstract

Current approaches to treating cancers often involve the use of drugs that are toxic to both cancer cells and normal cells. Over the past decade, advances have been made in understanding the genetic changes underlying the transformation of normal cells into cancerous cells that has led to treatment models that would selectively target the cancer cells. It has been found that cancer cells with mutations in p53 that are exposed to DNA damage are hypersensitive to agents that inhibit the G2 checkpoint.

To find novel G2 checkpoint inhibitors, mitotic ELISA assays were used to screen 1500 marine bacterial and sponge extracts. Four G2 checkpoint inhibitors were isolated and identified: staurosporine and its oxazolidone derivative, debromohymenialdisine and isogranulatimide. It was found that debromohymenialdisine and isogranulatimide induce entry into mitosis and this is dependent on the activation of cdc25 phosphatase and cdc2 kinase.

To gain a better understanding of the G2 checkpoint pathway, attempts were made to identify the *in vivo* targets of debromohymenialdisine and isogranulatimide by affinity chromatography, overlay assays and immunocytochemistry, without success. However, *in vitro* kinase assays have shown that debromohymenialdisine and isogranulatimide potently inhibit the kinase GSK-3 β . Further studies involving β -catenin, a key downstream component of GSK-3 β , provided evidence that the compounds inhibit GSK-3 β *in vivo* as well. The results suggest that GSK-3 β and β -catenin may play a yet unidentified role in the G2 checkpoint pathway.

Table of Contents

Abstract	ii
Table of Contents	iii
List of Figures	vii
List of Abbreviations	ix
Acknowledgements	xi

Chapter 1 Introduction

1.1 Cell cycle	1
1.2 Cell cycle checkpoints	5
1.3 G1 checkpoint	7
1.4 G2 checkpoint	8
1.5 G2 checkpoint inhibitors in cancer therapy	14
1.6 G2 checkpoint inhibitors as tools in cell cycle research	19
1.7 Research objectives	19

Chapter 2 Material and Methods

2.1 Cell culture	22
2.2 Flow cytometry	22
2.3 Drug screening of marine extracts for G2 checkpoint inhibitors	23
2.4 Mitotic ELISA	23
2.5 Mitotic index	24

2.6 Cdc2 immunoprecipitation and kinase assay	25
2.7 Western blotting	26
2.8 Immunofluorescence	26
2.9 Preparation of nuclear extracts	27
2.10 Production and purification of recombinant GSK-3 β	28
2.11 GSK-3 β phosphotransferase assay	29

Chapter 3

Identification of G2 checkpoint inhibitors debromohymenialdisine and isogranulatimide

3.1 Initial screen of 1500 marine extracts	30
3.2 Activity profiles of debromohymenialdisine and isogranulatimide	32

Investigation of the mechanism of action of debromohymenialdisine and isogranulatimide

3.3 Effects of debromohymenialdisine and isogranulatimide on Cdc2 kinase	34
3.3a Debromohymenialdisine and isogranulatimide stimulate the dephosphorylation of Cdc2	36
3.3b Debromohymenialdisine and isogranulatimide cause an increase in Cdc2 kinase activity	37
3.4 Debromohymenialdisine and isogranulatimide require the activation of a tyrosine phosphatase	40

3.5 Identifying in-vivo targets of debromohymenialdisine and isogranulatimide	42
3.5a Coupling debromohymenialdisine to a solid support	42
3.5b Radiolabeling of isogranulatimide with ^{125}I	42
3.6 Effects of checkpoint inhibitors on the abundance and subcellular localization of cell cycle regulatory proteins	43
3.6a Cyclin A	45
3.6b Cyclin B	45
3.6c Cyclin-dependent kinases: p33 ^{cdk2} and p34 ^{cdc2}	50
3.6d Phosphatases: cdc25B and cdc25C	50
3.6e Wee1	58
3.6f 14-3-3	58
3.7 Debromohymenialdisine and isogranulatimide are in vitro inhibitors of GSK-3 β	62
3.8 Evidence for in vivo inhibition of GSK-3 β by debromohymenialdisine and isogranulatimide	64
3.8a Debromohymenialdisine and isogranulatimide cause an increase in intracellular abundance of β -catenin	64
3.9 Effect of irradiation and checkpoint inhibitors on subcellular localization of GSK-3 β	69

Chapter 4 Discussion

4.1 Identification of novel G2 checkpoint inhibitors,	71
---	----

debromohymenialdisine and isogranulatimide	
4.2 Debromohymenialdisine and isogranulatimide act upstream of cdc2 and require the activation of a tyrosine phosphatase likely to be cdc25C	72
4.3 Identifying the in-vivo targets of debromohymenialdisine and isogranulatimide	73
4.4 Debromohymenialdisine and isogranulatimide are in vitro inhibitors of GSK-3 β	78
4.5 Future directions	81
4.6 Conclusion	81
References	83

List of Figures

Figure 1.	Cell cycle and DNA damage checkpoints	2
Figure 2.	Positive and negative regulation of Cdc2 kinase	6
Figure 3.	G1 checkpoint pathway	9
Figure 4.	Current model of the mammalian G2 checkpoint pathway	11
Figure 5.	Overview of G2 checkpoint pathway in fission yeast <i>S. pombe</i>	13
Figure 6.	Rationale for use of G2 checkpoint inhibitors in cancer therapy	16
Figure 7.	Structures of known G2 checkpoint inhibitors	18
Figure 8.	Mitotic ELISA assay	20
Figure 9.	Cell cycle profile of G2 arrest in MCF-7 mp53 cells	31
Figure 10.	Structures of G2 checkpoint inhibitors isolated from marine extracts	33
Figure 11.	G2 checkpoint inhibition profile of debromohymenialdisine and isogranulatimide	35
Figure 12.	Effect of G2 checkpoint inhibitors on the phosphorylation of p34 ^{cdc2}	38
Figure 13.	Cdc2 kinase activity in response to checkpoint inhibitors	39
Figure 14.	Inhibition of debromohymenialdisine and isogranulatimide by phenylarsine oxide	41
Figure 15.	Nuclear/cytoplasmic distribution of cyclin A	46

Figure 16.	Nuclear/cytoplasmic distribution of cyclin B	48
Figure 17.	Nuclear/cytoplasmic distribution of cdk2	51
Figure 18.	Nuclear/cytoplasmic distribution of cdc2	53
Figure 19.	Nuclear/cytoplasmic distribution of cdc25B	55
Figure 20.	Nuclear/cytoplasmic distribution of cdc25C	56
Figure 21.	Nuclear/cytoplasmic distribution of wee1	59
Figure 22.	Nuclear/cytoplasmic distribution of 14-3-3	60
Figure 23.	Debromohymenialdisine and isogranulatimide in vitro inhibition of GSK-3 β kinase activity	63
Figure 24.	Nuclear/cytoplasmic distribution of β -catenin	66
Figure 25.	Nuclear localization of β -catenin in response to G2 checkpoint inhibitors	68
Figure 26.	Nuclear/cytoplasmic distribution of GSK-3 β	70

List of Abbreviations

ABTS	2,2'-azino-bis(3-ethylbenzthiazalone-6-sulfonic) acid
ATM	ataxia telangiectasia
ATP	adenosine triphosphate
CDK	cyclin-dependent kinase
cpm	count per minute
DBH	debromohymenialdisine
DMEM	Delbecco's Modified Eagle Medium
DTT	dithiothreitol
EGTA	ethylene-bis(β -aminoethylether)N,N,N',N'-tetraacetic acid
ELISA	enzyme-linked immunosorbent assay
FBS	fetal bovine serum
GSK	glycogen synthase kinase
HPLC	high pressure liquid chromatography
HRP	horseradish peroxidase
Igran	isogranulatimide
IPTG	isopropyl β -D-thiogalactopyranoside
LB	Luria-Bertani
mp53	mutated in p53
NMR	nuclear magnetic resonance

PAGE	polyacrylamide gel electrophoresis
PAO	phenylarsine oxide
PBS	phosphate-buffered saline
PI3	phosphatidylinositol 3
PMSF	phenylmethylsulfonyl fluoride
Rb	retinoblastoma
SDS	sodium dodecyl sulfate
TBS	Tris-buffered saline
Tris	Tris(hydroxymethyl)aminomethane

Acknowledgements

Welcome to the one page where I give thanks to all those who have helped achieve my goals. First and foremost I would like to thank the Lord for His wisdom and guidance. Many thanks go to Michel for accepting me into his lab. His enthusiasm for research was both contagious and inspiring. Thanks to my committee members Dr. Ross MacGillivray and Dr. Ray Andersen for their support. Thanks to Hilary for all her help, advice and morning chats. Thanks to the members of my lab past and present, Lili, Lynette, Xiuxian, Pat, Daisy, Cristina, members of Macintosh's lab and others for their friendships, which won't be forgotten. Thanks to Lawrence for the never-ending supply of chilled H₂O. This thesis is dedicated to my family, my father Stjepan, my mother Luce, my brother Denis, my sister Monika and her family. Special thanks go to my future mother-in-law and father-in-law, Suzanne and Michael Nemeth for their unwavering support. Finally, to my fiancé Andrea, thank you. Thanks for always being there for me, encouraging me, putting up with my seminar rehearsals, making me smile when things were down and sharing in my joys when things were going good. Thank you Andrea and I love you. I would like to close off with a few words from Lord Tennyson.

“Made weak by time and fate, but strong in will
To strive, to seek, to find and not to yield.”

Chapter 1

Introduction

1.1 Cell cycle

The eukaryotic cell cycle is a tightly controlled series of events that ensures the continuous growth of cells and the faithful propagation of genetic information to daughter cells. Breakdown of cell cycle regulation often leads to the accumulation of genetic lesions that can cause unchecked proliferation, altered phenotype or cell death.

The eukaryotic cell cycle can be divided into two major phases, M phase and interphase. M phase includes the process of mitosis, during which duplicated chromosomes are separated into two nuclei, and cytokinesis, during which the cell divides into two daughter cells. During interphase, the cell undergoes the processes of growth and replication of DNA. Interphase can be further divided into three stages. The first stage, G1 or Gap1 phase of the cell cycle starts at the conclusion of mitosis and ends with the onset of DNA synthesis. The second stage is the S phase during which the cell replicates its DNA. The G2 phase is the second gap phase that begins upon the completion of DNA replication and ends with the onset of mitosis (figure 1).

Progress through the cell cycle is regulated by a number of positive and negative regulatory phosphorylation and dephosphorylation events involving protein phosphatases, protein kinases, including cyclin-dependent kinases (CDK) and their cyclin regulating subunits, and cyclin-dependent kinase inhibitors. CDKs controls the cell cycle by

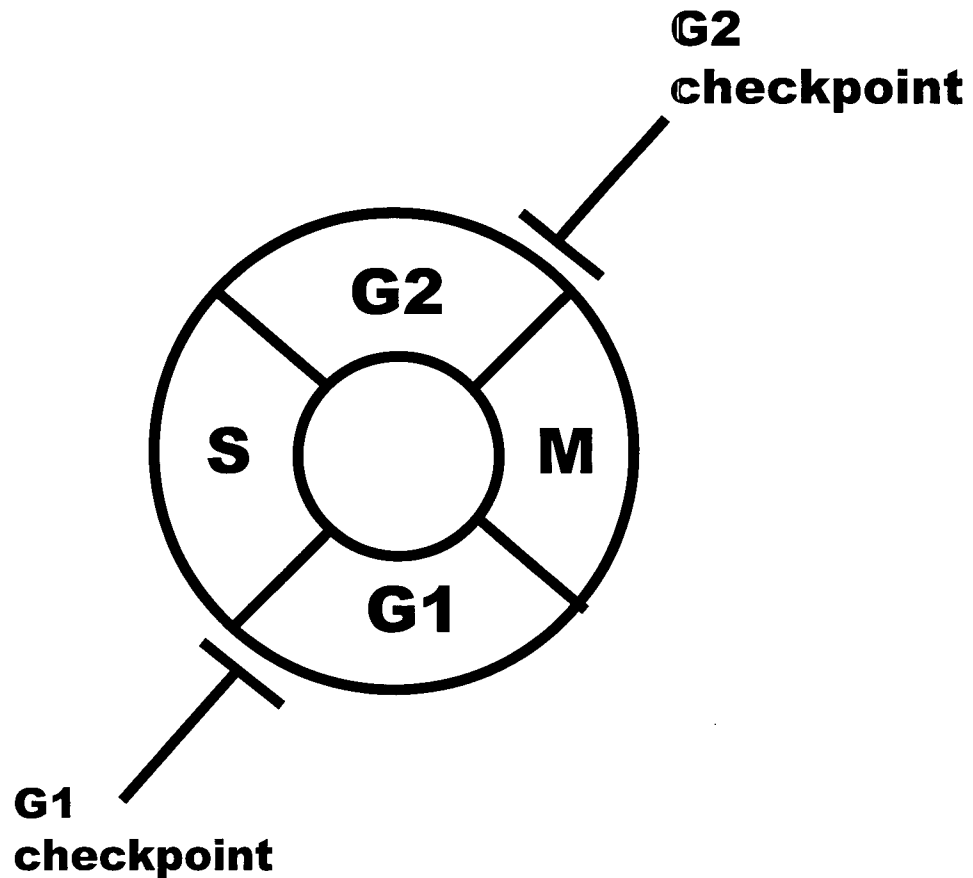


Figure 1. Cell cycle and DNA damage checkpoints

The cell cycle can be divided into four stages. Interphase is composed of the gap stages G1 and G2 when cellular growth occurs and the S phase when the DNA is replicated. The M phase involves the cellular processes involved in the division of the cell into two daughter cells. The cell cycle is regulated by two DNA damage checkpoints. If cells have been exposed to DNA damage, the G1 checkpoint regulates entry into S phase and the G2 checkpoint regulates entry into mitosis.

phosphorylation of key substrates within the cells. Cyclins modulate the activity of CDKs by binding and directing them to their substrates at specific phases of the cell cycle. The expression of cyclins is periodic with different cyclins expressed at different cell cycle phases.

Transition through the G1 phase requires the activity of cyclin D and its CDK partners, CDK4 and CDK6. The activity of cyclin D/CDK4 and CDK6 is first detected at mid G1 phase and reaches a maximum at the G1-S phase transition. The cyclin D/CDK are believed to commit the cell to G1-S phase transition by phosphorylation of the retinoblastoma (Rb) gene product (Reviewed in Hatakeyama and Weinberg, 1995). Rb controls gene expression mediated by members of the E2F family of heterodimeric regulators. When Rb is hypophosphorylated, it binds to E2F protein repressing the expression of E2F's target genes. However when Rb is hyperphosphorylated, E2F is released from the complex, allowing the expression of E2F responsive genes (Weintraub *et al*, 1992). The hyperphosphorylation of Rb is first initiated by the cyclin D dependent kinases but is maintained by the activity of cyclin E and its catalytic subunit CDK2 (Hatekayama *et al.*, 1994).

E2F proteins act as transactivators of genes that are essential for entry and progression through the S phase (Nevins, 1992). To commit the cell to the G1-S phase transition, E2F can stimulate the expression of cyclin E, cyclin A and E2F. This establishes a positive feedback loop that promotes the phosphorylation of Rb by cyclin E/CDK2 and as a result, the cells become irreversibly committed to the G1-S phase transition (Sherr, 1996). E2F can also transactivate the expression of genes that are required for the S phase including DNA polymerase-alpha, dihydrofolate reductase and

thymidine kinase. In addition, E2F activates the expression of *cdc25C* and *cdc2* which are required for entry into mitosis (Kaelin *et al.*, 1997).

After cells have entered the S phase, the timely inactivation of cyclin E and E2F activity may be a crucial requirement for cell cycle progression (Sherr, 1996). This is achieved in part by CDK2 which can phosphorylate cyclin E at a site which targets it for degradation by the ubiquitin proteasome pathway (Won and Reed, 1996). Cyclin A/Cdk2 can inactivate E2F by phosphorylation on one of its heterodimeric components which prevents DNA binding (Krek *et al.*, 1995). Cyclin A/CDK2 is also believed to phosphorylate proteins whose activities are implicated in regulating the initiation of DNA replication. They include substrates that are involved in origin-recognition complex (ORC) and CDC6 which are involved in the assembly of the preinitiation complex (Stillman, 1996).

During late S phase, the expression of cyclin B1 begins and reaches a peak in late G2 phase and early mitosis. Cyclin B1 interacts with $p34^{cdc2}$ to form the Cdc2 kinase whose activity is required for entry into mitosis (Pines, 1993). Cdc2 activity is regulated by association of its $p34^{cdc2}$ catalytic subunit with cyclin B1, a positive regulatory subunit and by reversible phosphorylation. In addition to cyclin B1 binding, complete activation of Cdc2 requires phosphorylation at Thr161 which is carried out by the CDK-activating kinase (CAK, Lew and Kornbluth, 1996). During the G2 phase, the expanding population of cyclin B1/ $p34^{cdc2}$ is held in an inactive state by inhibitory phosphorylations at Thr14 and Tyr15 to prevent premature activation. In human cells, kinase wee1 was found to phosphorylate $p34^{cdc2}$ at Tyr15 (McGowan *et al.*, 1993, Parker *et al.*, 1992)

whereas kinase Myt1 was found to phosphorylate it at both Thr14 and Tyr15 (Mueller *et al.*, 1995, Liu *et al.*, 1997).

At the end of G2, rapid dephosphorylation of the inhibitory sites on p34^{cdc2} leads to the complete activation of the intracellular pools of Cdc2 causing entry into mitosis. The stimulation of Cdc2 kinase activity is thought to be triggered by both the inactivation of wee1 and myt1 kinases and by the activation of the dual-specificity phosphatases, cdc25B and cdc25C. It is not clear precisely what role cdc25B or cdc25C play in causing entry into mitosis but evidence suggests that cdc25B acts as a “starter phosphatase”, dephosphorylating the inhibitory sites on p34^{cdc2} which activates Cdc2 (Lammer *et al.*, 1998). Activated Cdc2 can phosphorylate cdc25C at sites which stimulates its ability to dephosphorylate Cdc2 thus creating a positive feedback loop (Hoffmann *et al.*, 1993). These processes ensure that there is a complete and irreversible activation of Cdc2 and consequently the cells become committed to entry into mitosis (figure 2).

Activated Cdc2 initiates the events of mitosis by phosphorylating a number of substrates. Cdc2 can directly phosphorylate the nuclear lamins which leads to the breakdown of the nuclear envelope. Cdc2 also phosphorylates histone H1 which may enhance the condensation of chromosomes. In addition, Cdc2 has been shown to control the mitotic microtubule arrays (Reviewed in Nigg, 1993).

1.2 Cell cycle checkpoints

The ability of eukaryotic cells to maintain genomic integrity is vital for cell survival and proliferation. The inability to maintain genomic stability would result in mutations that could lead to cell death or give rise to cancers. There are built-in

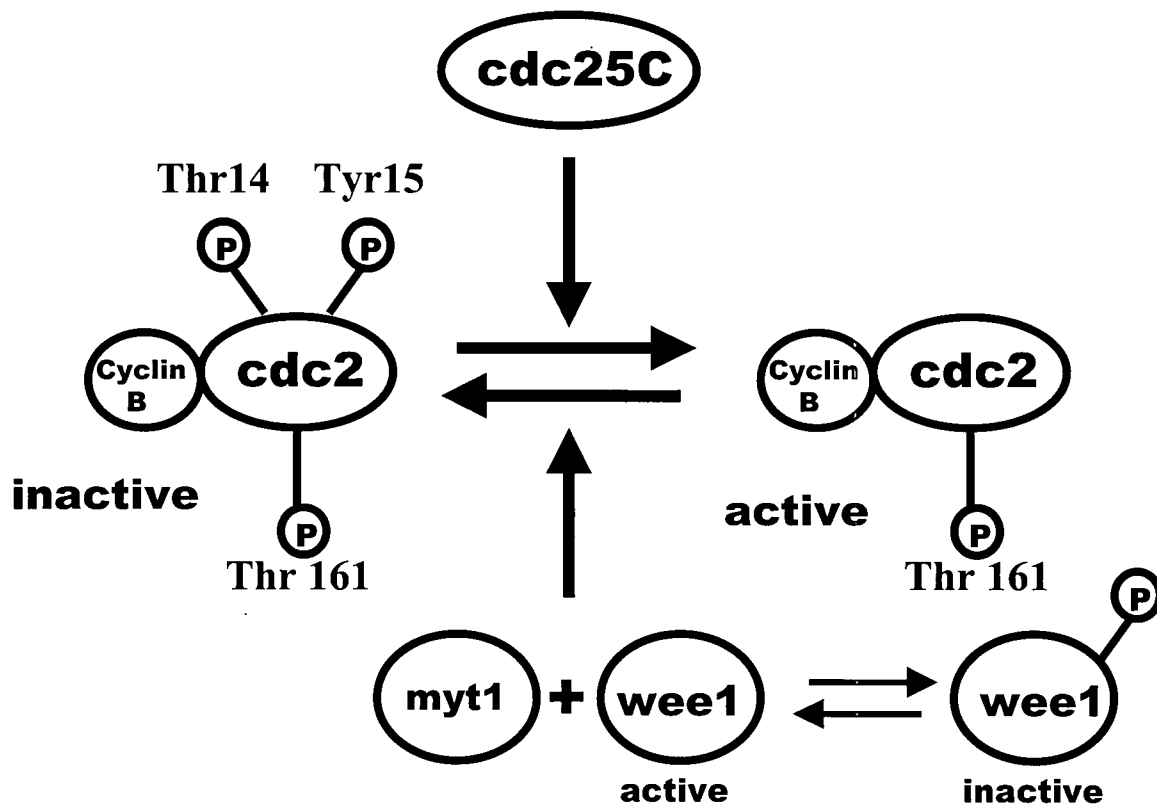


Figure 2. Positive and negative regulation of Cdc2 kinase

Activation of cdc2/cyclinB requires phosphorylation on Thr 161 by CDK-activating kinase and the dephosphorylation at residues Thr14 and Tyr15 by cdc25C phosphatase. Cdc2/cyclinB is inhibited by phosphorylation at Thr14 and Tyr15 by the kinases wee1 and myt1. The activity of wee1 and cdc25C is itself controlled by phosphorylation.

mechanisms known as checkpoints employed by the cell to protect itself from the harmful effects of DNA damage. When checkpoints are activated by DNA damage, a signal cascade is elicited which causes a transitory halt in cell-cycle progression. It is believed that this allows time for DNA repair to occur in order to prevent the replication of damaged DNA templates and segregation of broken chromosomes (Kaufmann and Paules, 1996).

After cells have been exposed to DNA damage, they can arrest at either the G1 phase or the G2 phase, depending on which position of the cell cycle they are in. The G1 checkpoint functions to prevent entry into the S phase and the G2 checkpoint prevents entry into mitosis from G2 (figure 1).

1.3 G1 checkpoint

DNA damage triggers several signal transduction pathways that lead to DNA repair coupled with a halt in cell-cycle progression or to apoptosis (programmed cell death), depending on the severity of DNA damage. The G1 checkpoint signaling cascade is mediated by the transcription factor p53 whose activity rises after DNA damage. This is achieved in part by the stabilization of p53, which is normally rapidly degraded, and in part by an increase in p53 transactivation activity (Levine, 1997).

The mechanism by which DNA damage is detected and signaled to p53 remains unclear but evidence implicates the kinases ATM and ATR (Lakin *et al.*, 1999). The stimulation of p53 by DNA damage is believed to be mediated by the gene product of the ATM gene (Canman *et al.*, 1998), a 370 kD protein kinase with a COOH terminal domain similar to the catalytic subunit of phosphoinositide 3-kinase (Savitsky *et al.*,

1995). Mutations in the ATM gene cause a wide variety of cellular defects including acute sensitivity to radiation, genomic instability and the inability to activate cell cycle checkpoints (Lavin and Shiloh, 1997; Shiloh and Rotman, 1997). A structurally related kinase, ATR has also been shown to mediate the activity of p53 (Lakin *et al.*, 1999). ATM and ATR are believed to act as sensors recognizing DNA damage and transducing the signal to p53.

ATM and ATR can phosphorylate p53 in vitro at Ser15 which is phosphorylated in vivo in response to DNA damage (Banin *et al.*, 1998, Waterman *et al.*, 1998, Lakin *et al.*, 1999). The phosphorylation of p53 at Ser15 leads to the stabilization of p53 by inhibiting its interaction with Mdm2, a protein that targets p53 for degradation via the ubiquitin-proteasome pathway (Prives, 1998). The increase in intracellular pools of p53 causes an increase in its activity as a transcription factor stimulating the transcription of downstream effector genes. The most notable of these genes is p21^{CIP1}, which inhibits the kinase activity of various cyclin/CDK complexes that are involved in the transition to S phase, including cyclinA/CDK2 (Dulic *et al.*, 1994, Xiong *et al.*, 1993). As a result, the Rb protein remains hypophosphorylated and cells are unable to enter the S phase, leading to G1 cell cycle arrest (figure 3).

1.4 G2 checkpoint

The ultimate downstream target for the mammalian G2 checkpoint pathway is the Cdc2 kinase. After DNA damage, Cdc2 is maintained in its inactive phosphorylated state to prevent the cell from entering mitosis. A key component of the G2 checkpoint pathway has been identified, the Chk1 kinase. In response to DNA damage, Chk1 is

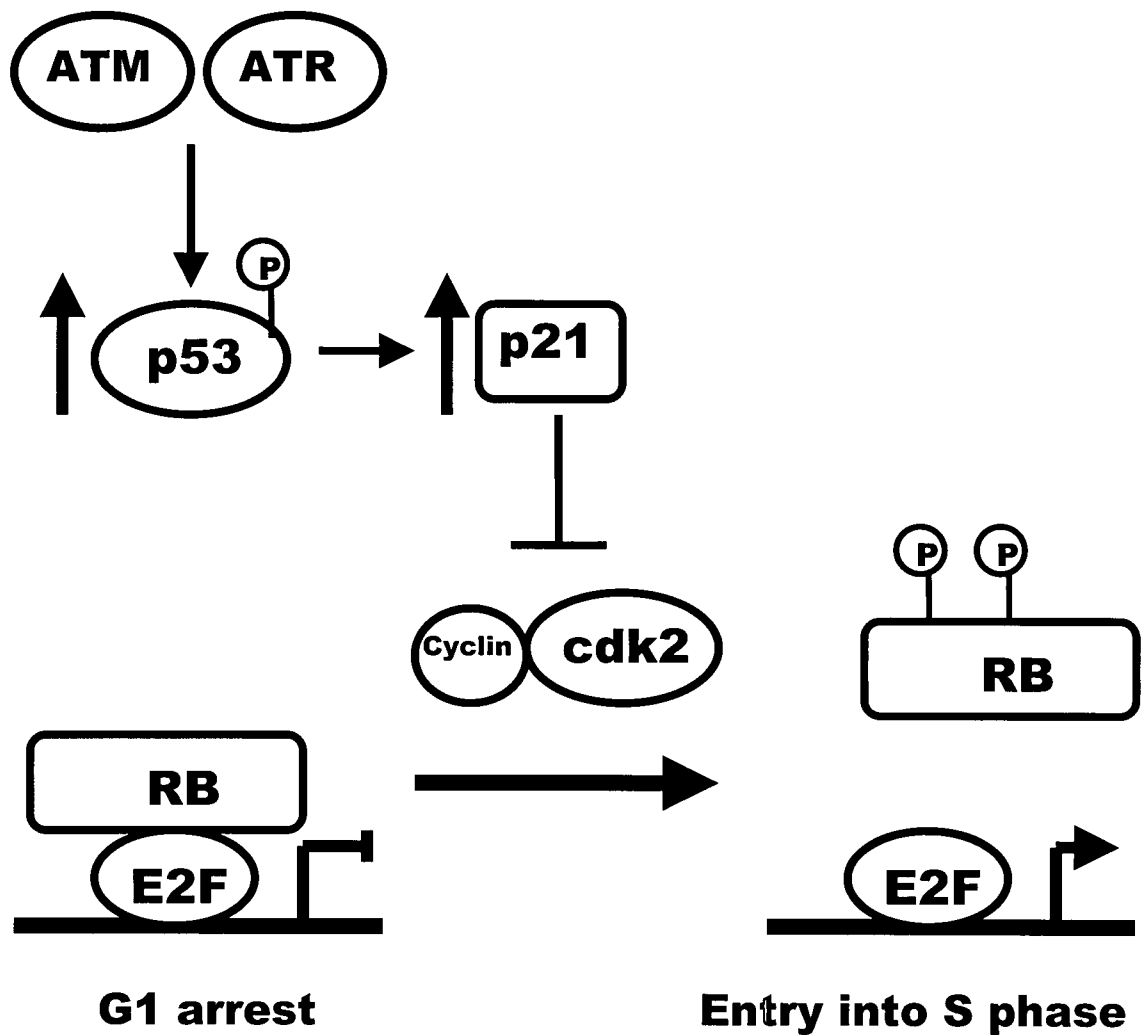


Figure 3. The G1 Checkpoint pathway

After exposure to DNA damage, intracellular p53 levels increase resulting in the activation of expression of p21 protein. p21 inhibits the function of cyclin/cdk2 which is to phosphorylate RB. RB remains hypophosphorylated resulting in inability to enter S phase and consequently G1 arrest.

activated and phosphorylated in an ATM-dependent manner (Chen *et al.*, 1997). Chk1 is believed to inhibit the Cdc2 kinase via the regulation of wee1 (Connell *et al.*, 1997) and cdc25C (Sanchez *et al.*, 1997).

Chk1 is believed to inactivate Cdc2 by two different mechanisms. First it has been demonstrated by O'Connell *et al* (1997) that in fission yeast, Chk1 can directly phosphorylate wee1 in vitro. In addition, they have demonstrated that wee1 is required for cell cycle arrest induced by overexpression of Chk1. These observations suggest that in response to DNA damage wee1 is phosphorylated and activated by Chk1 in vivo and this results in the inhibition of the Cdc2 kinase. Alternatively, Chk1 has been found to phosphorylate cdc25C at Ser216, enhancing its binding to 14-3-3 proteins which is believed to target cdc25C for nuclear export (Peng *et al.*, 1997, Dalal *et al.*, 1999). Therefore after DNA damage, cdc25C becomes cytoplasmic and sequestered away from its nuclear substrate Cdc2. Cdc2 remains inactive and phosphorylated which leads to G2 arrest (figure 4).

Recent studies have shown that cells expressing a non-phosphorylatable Thr14 and Tyr15 mutant form of Cdc2 have a reduced but still substantial G2 arrest (Jin *et al.*, 1996). This suggests mechanisms other than inhibitory phosphorylation of Cdc2 may exist to cause G2 arrest. One such mechanism could be the regulation of cyclin B1's intracellular localization in response to DNA damage. In order for cells to enter mitosis, cyclin B1 needs to be translocated into the nucleus in order to initiate downstream mitotic events (Pines and Hunter, 1991, Ookata *et al.*, 1992). Smeets *et al* (1994) have found that cyclin B1 remains cytoplasmic in cells that have been arrested in G2 by DNA damage. In addition, cells expressing a mutant form of cyclin B1 that targets it to the nucleus in all

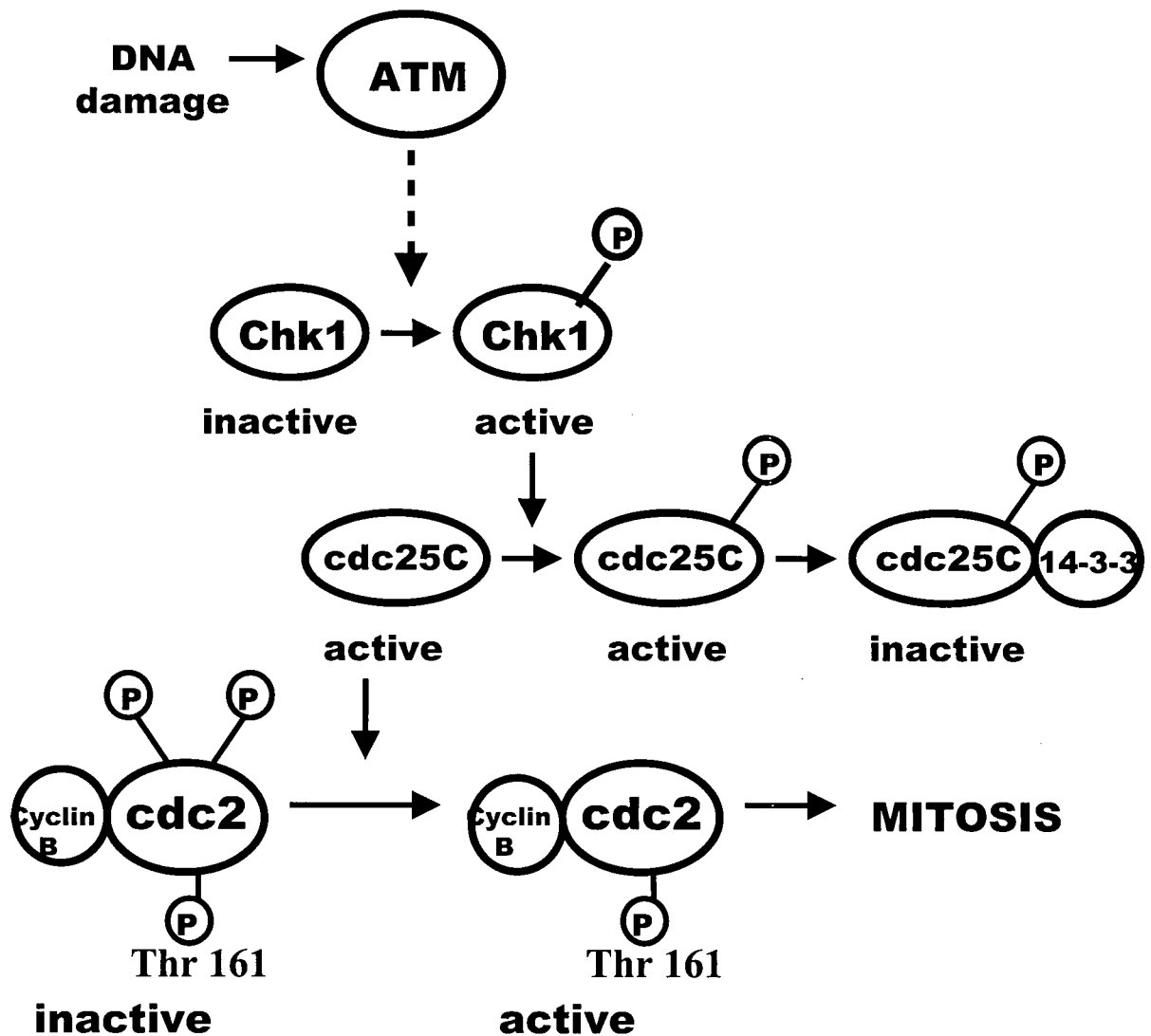


Figure 4. Current model of the mammalian G2 checkpoint pathway

ATM acts as a sensor recognizing DNA damage and initiating a signal cascade that results in the phosphorylation and activation of the checkpoint kinase, Chk1. Activated Chk1 phosphorylates cdc25C at residue S216 that is believed to mediate binding to 14-3-3 resulting in functional inactivation of the complex. Inactive cdc25C fails to activate cdc2 causing arrest in G2. The broken arrows between ATM and Chk1 indicate that ATM activates Chk1 by means that have yet to be elucidated.

cell cycle phases can partially override G2 arrest in response to DNA damage (Jin *et al.*, 1998). This suggests that DNA damage acts not only by stabilizing the inhibitory phosphorylations of Cdc2 but also by maintaining the cytoplasmic localization of cyclin B1.

In the mammalian G2 checkpoint pathway, the signaling pathway upstream of Chk1 remains little understood. What is known is that Chk1 is phosphorylated and activated in an ATM-dependent manner (Chen *et al.*, 1997). How the signal is propagated from ATM to Chk1 is unclear but clues can be provided by genetic studies in yeast *S. pombe* which also has a G2 checkpoint pathway.

The organization of the checkpoint pathway downstream of Chk1 in *S. pombe* is similar to that in mammalian cells (Reviewed in Rhind and Russell, 1998). The components upstream of chk1 are believed to involve a group of proteins rad1, rad3, rad9, rad17, rad26 and hus1 that are required for cell cycle arrest in response to DNA damage (Al-Khodairy and Carr, 1992; Rowley *et al.*, 1992). These proteins are involved in the recognition of DNA damage and the transduction of the checkpoint signal to chk1. The nature of the interaction between chk1 and the rad proteins remains unclear but it is believed that a protein Crb2, phosphorylated in response to DNA damage, may act as a mediator between chk1 and the rad proteins (figure 3; Saka *et al.*, 1997). Putative human homologues of various upstream components of yeast checkpoint proteins have been identified including hRad1, hRad9, hRad17 and hHus1 (Parker *et al.*, 1998; Kostrub *et al.*, 1998; Lieberman *et al.*, 1996; Parker *et al.*, 1998). However, the roles of these proteins in mammalian checkpoint response have yet to be determined.

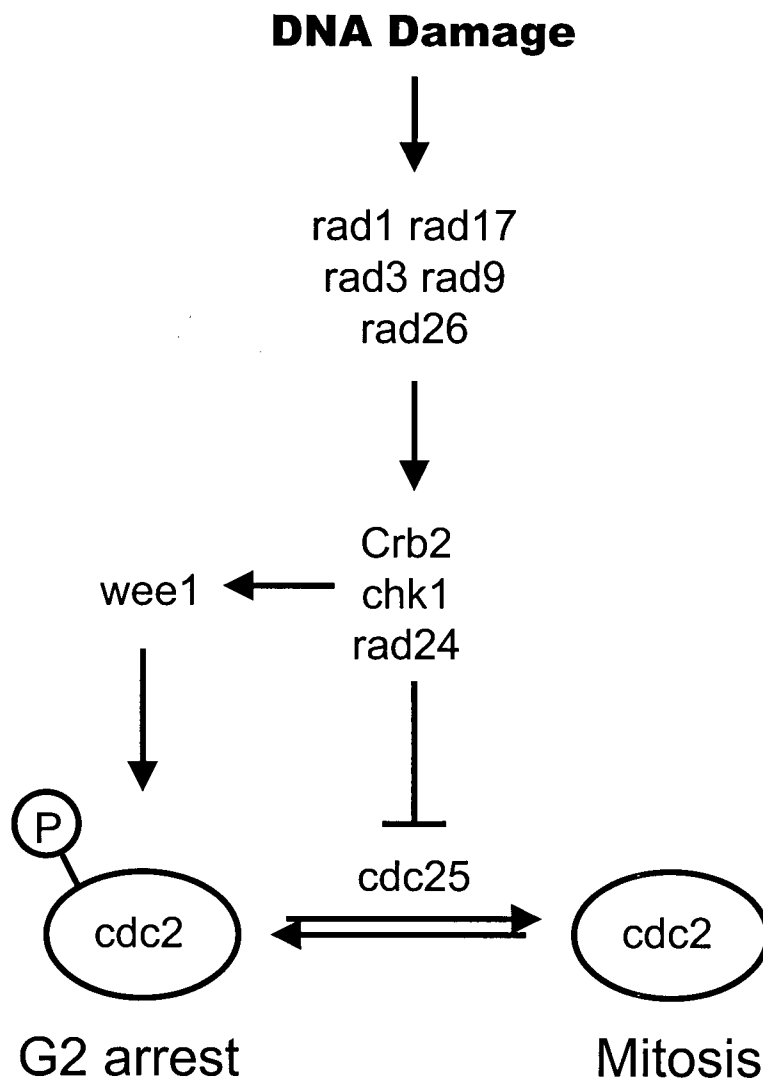


Figure 5. Overview of G2 checkpoint pathway in fission yeast *S. pombe*

DNA damage is sensed by a number of proteins including rad1, rad17, rad3, rad9 and rad26. These proteins stimulate the activation of chk1 possibly by stimulation of Crb2. Chk1 along with rad24 inhibits the cdc2 kinase via the inhibition of the phosphatase cdc25 and the activation of the kinase wee1.

1.5 G2 checkpoint inhibitors in cancer therapy

Cancer can be defined as a disease characterized by an abnormal cellular growth and the ability to invade normal tissues and metastasize to distinct sites. Treatment of cancers often involves the use of anti tumor drugs that have a wide variety of cellular effects. They may be drugs that have anti-proliferative effects by interfering with mitotic microtubule function or they may be cytotoxic agents by binding to or damaging DNA or inhibiting nucleic acid synthesis. One drawback of these classes of compounds is that not only do they kill cancerous cells but they are also harmful to normal cells limiting their effectiveness in eradicating tumors.

However, over the past 20 years numerous advances have been made into understanding the genetic changes underlying the transformation of normal cells into cancerous cells. A search has been undertaken for newer and more effective chemotherapeutic agents that would selectively target these genetic differences. One of the most common genetic mutations, found in over 60% of cancers is the loss of p53 function (Greenblatt *et al*, 1994). The loss of p53 leads to the cell's inability to activate the G1 checkpoint in response to DNA damage. This mutation is believed to lead to increased genomic instability and proliferation which are hallmarks of cancers.

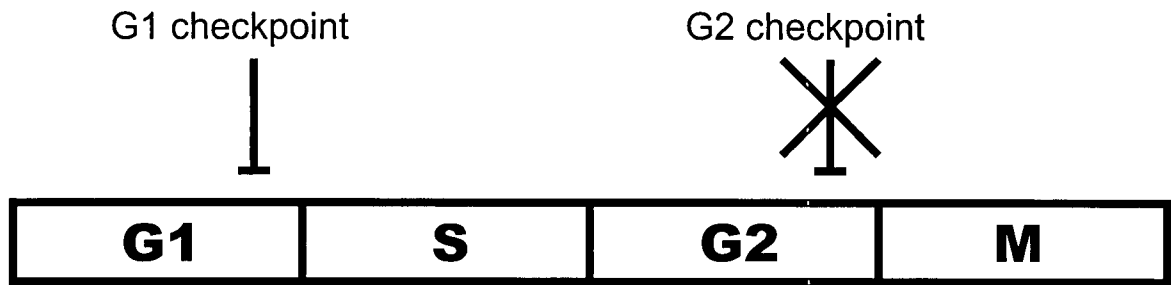
One approach to treating cancers that have mutated p53 involves the introduction of WT p53 into cancer cells by gene therapy. It is hoped that this would restore the cell's ability to undergo apoptosis which is dependent on p53. However there are currently serious limitations to this approach as the genes have to be injected directly into the tumor limiting their usefulness to solid tumors and not to cancers that may have metastasized (Barinaga, 1997). An alternative approach is to take advantage of the loss

of p53 function to kill cancer cells with mutated p53 by introducing a genetically modified adenovirus. This human respiratory virus requires the disabling of p53 function in order to infect and kill the host cell because the p53 gene activity prevents viral replication. Removal of the viral gene responsible for disabling p53 from the adenovirus would allow it to infect and kill only cells with mutated p53. This treatment has showed some success but it requires that the adenovirus be directly injected into a solid tumor in order to be effective (Pennis, 1996). Again, this approach limits its use for metastatic cancer.

Cancer cells with mutations in p53 have lost the ability to activate the G1 checkpoint. It may be possible to exploit this by treating tumor cells with mutated p53 with agents that prevent the activation of the G2 checkpoint and exposing them to DNA damage. The tumor cells would be unable to arrest at either checkpoint and as a result, would enter mitosis with extensive DNA damage leading to cell death. On the other hand, normal cells exposed to DNA damage and G2 checkpoint inhibitors would still be able to arrest at the G1 checkpoint to repair damaged DNA, resulting in increased cell survival over cells with mutated p53 (figure 6).

This principle has been demonstrated in vitro: using a variety of paired cell lines differing in their p53 status, several groups have shown selective sensitization of cells with mutated p53 to treatment with DNA damage and G2 checkpoint inhibitors (Powel *et al*, 1995, Fan *et al*, 1995, Wang *et al*, 1996). A number of G2 checkpoint inhibitors have been discovered but they remain unsuitable for use in chemotherapy because they exhibit a wide variety of side effects. The most notable is 7-hydroxystaurosporine (UCN-01, figure 7D) which is currently undergoing phase I clinical trials. However, UCN-01 has a

A. Wildtype p53 cell



B mp53 cell

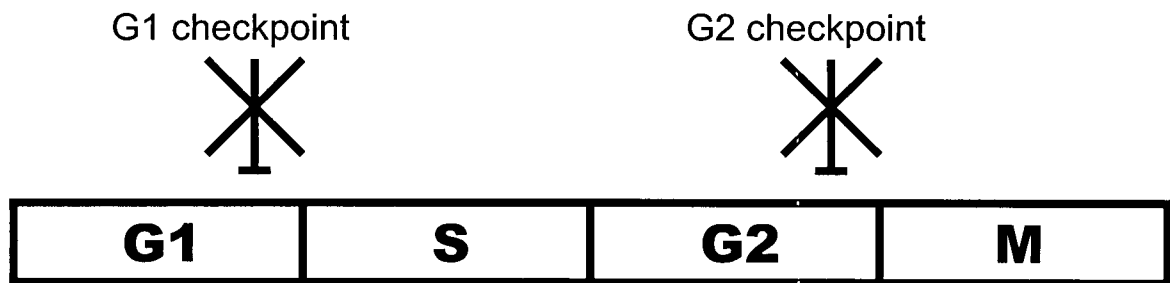


Figure 6. Rationale for use of G2 checkpoint inhibitors in cancer therapy

When cells with wildtype p53 are exposed to DNA damage and G2 checkpoint inhibitors, a large proportion will arrest at the G1 checkpoint to repair their DNA to enhance cell survival. Cells with mutated p53 exposed to the same conditions will be unable to arrest at either the G1 or the G2 checkpoint and will enter mitosis with DNA damage that will result in cell death

drawback in that it binds non-specifically to human α -acidic glycoprotein in the plasma, reducing its effectiveness in chemotherapy (Fuse *et al.*, 1999). Staurosporine is also a G2 checkpoint inhibitor (figure 7C), but it is a broad-based protein kinase inhibitor that has been demonstrated to have no antitumor activity in vivo (Akinaga *et al.*, 1991).

Other G2 checkpoint inhibitors that have been identified include the purine analogues, caffeine (figure 7A) and pentoxifylline (figure 7B). However, their numerous pharmacological effects preclude their effectiveness in chemotherapy (Arnaud, 1987). The protein phosphatase inhibitors, fostreicin (figure 7E) and okadaic acid (figure 7F) can also act as G2 checkpoint inhibitors (Roberge *et al.*, 1994). Their drawback is they can induce premature entry into mitosis in normal cells. Therefore, there is a need to find G2 checkpoint inhibitors that can act more specifically and can exert their effects at low concentrations to limit their cytotoxicity to normal cells.

Our laboratory has developed a high-throughput assay to rapidly screen for G2 checkpoint inhibitors (Roberge *et al.*, 1998). Marine extracts obtained from ascidians, sponges and bacteria were chosen as a source of potential compounds. Many of the marine organisms have evolved a vast array of structurally unique compounds used for defense, communication, and reproduction. Thus marine organisms provide an excellent source for novel compounds with biological activity (Rayl, 1999). Our assay involves the use of an MCF-7 epithelial breast cancer cell line that expresses a dominant negative mutant p53. The cells are subjected to ionizing radiation to induce DNA damage and become arrested in G2. Marine extracts are added and cells entering mitosis are quantified by ELISA using the TG-3 antibody which recognizes a phosphorylated form of nucleolin present only in mitotic cells (Anderson *et al.*, 1998). G2 checkpoint

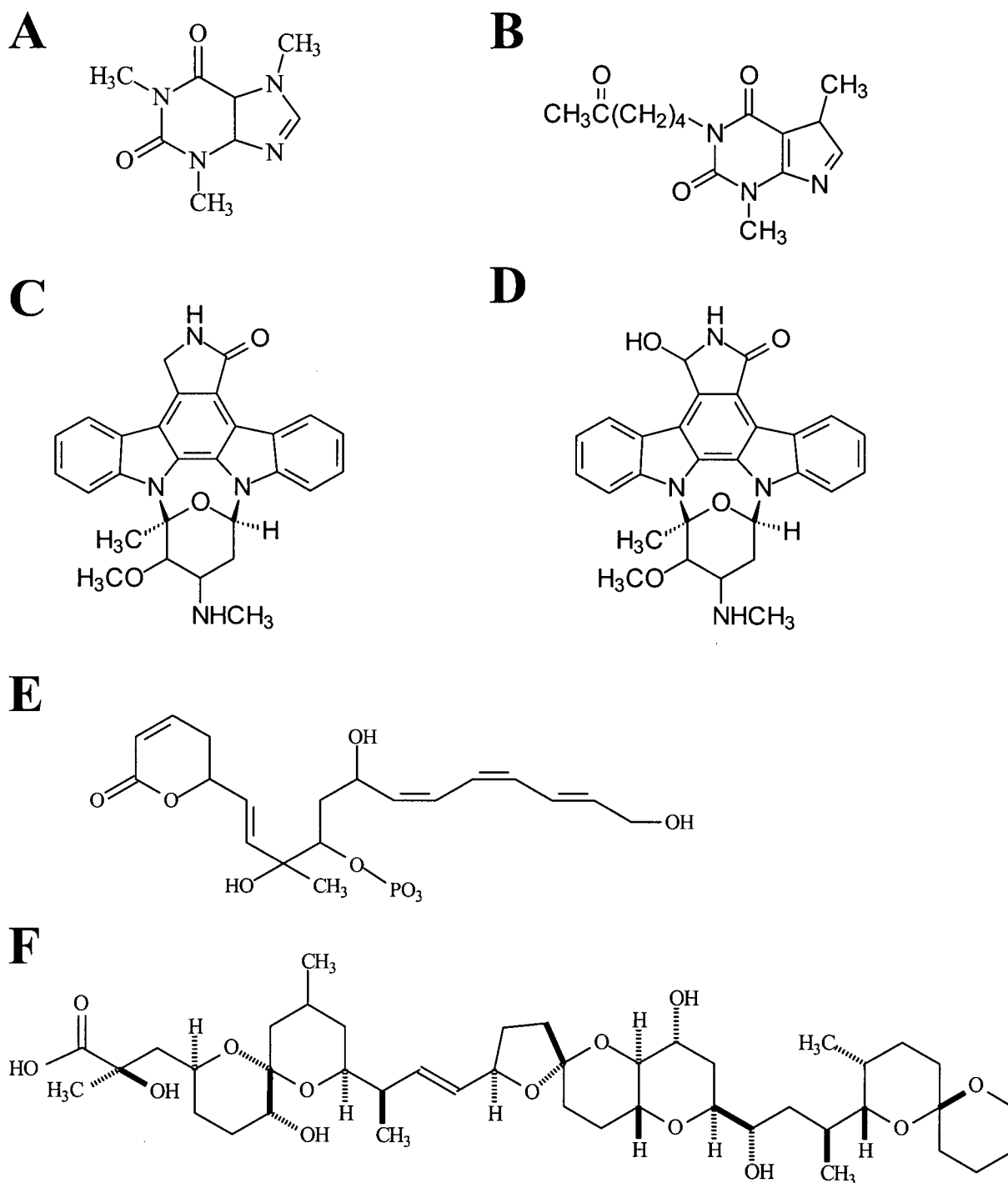


Figure 7. Structures of known G2 checkpoint inhibitors

Shown are caffeine (A) and its analogue pentoxifylline (B), the protein kinase inhibitors staurosporine (C) and UCN-01 (D), and the protein phosphatase inhibitors fostreicin (E) and okadaic acid (F)

inhibitors are purified from positive extracts using assay-guided fractionation and their structures are elucidated (figure 8).

1.6 G2 checkpoint inhibitors as tools in cell cycle research

As outlined before, much of our knowledge about the human G2 checkpoint pathway has been obtained by studying the equivalent pathway in yeast and then searching for the human homologues of yeast cell cycle proteins. However, it is clear that mammalian cells also have components not present in yeast. For example, the tumor suppressor protein p53 has no structurally related homologue in yeast. Therefore directly studying the G2 checkpoint pathway in mammalian cells is also needed. The novel G2 checkpoint inhibitors obtained from the screen described above can be used to gain a deeper understanding of the mechanisms of G2 arrest in mammalian cells. To address this, I have attempted to identify the potential *in vivo* targets of two novel G2 checkpoint inhibitors in order to better understand the G2 checkpoint pathway.

1.7 Research objectives

My project had three main objectives. The first was to participate in the isolation and identification of new G2 checkpoint inhibitors by using the assay developed in our laboratory to screen ~1500 marine extracts. I then to characterized the activity profile of the novel G2 checkpoint inhibitors.

The second objective was to characterize the mechanism of action of the inhibitors by studying their effect on known components of the G2 checkpoint pathway.

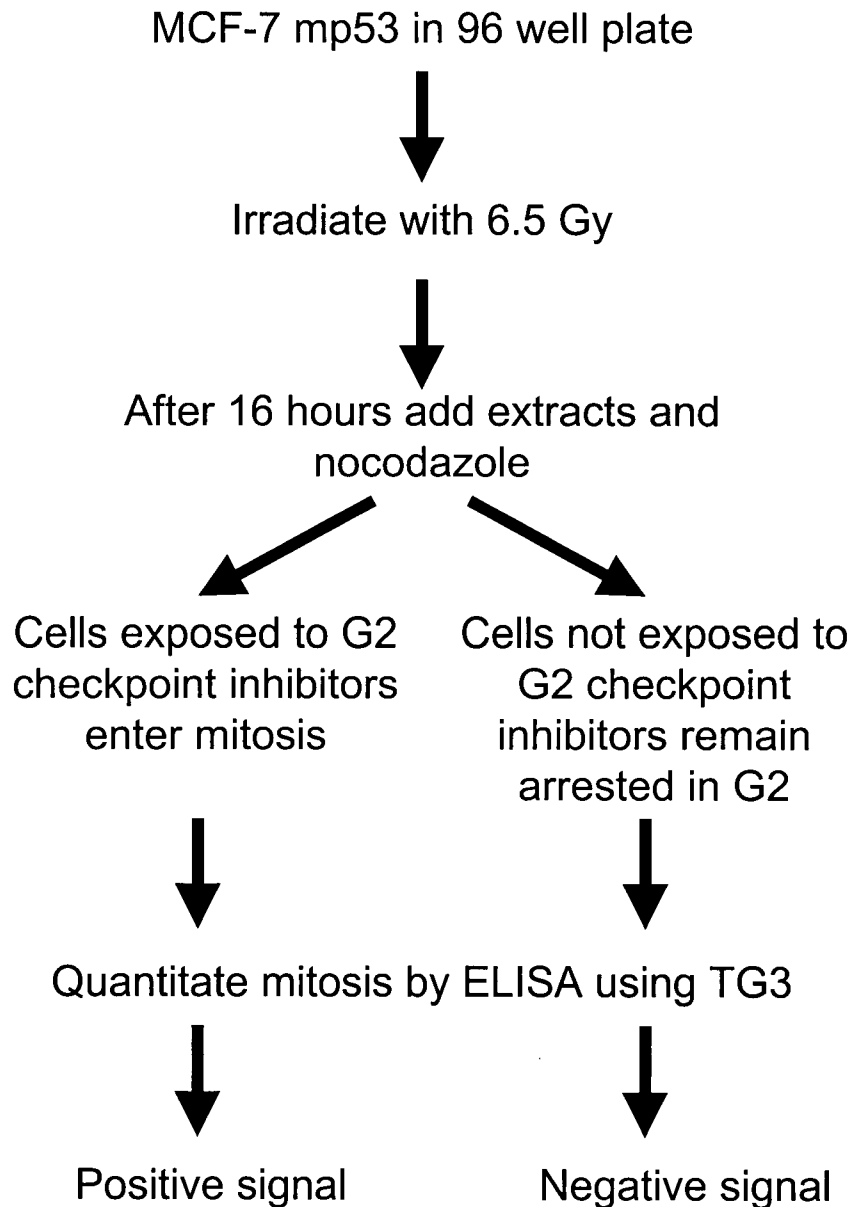


Figure 8. Mitotic ELISA assay

The assay used to efficiently screen for G2 checkpoint inhibitors is outlined. MCF-7 mp53 cells are plated in 96 well plates and exposed to 6.5 grays of γ -irradiation. After 16 hours, when cells are arrested in G2, extracts are added along with nocodazole for 6-8 hours. Cells exposed to a G2 checkpoint inhibitor will enter mitosis which is detected as a positive signal by ELISA using TG-3 antibody.

The final objective was to identify the direct targets of the G2 checkpoint inhibitors to reveal new components of the G2 checkpoint pathway.

Chapter 2

Materials and Methods

2.1 Cell culture

MCF-7 human mammary tumor cells expressing a dominant negative mutant p53 (Fan *et al.*, 1995) were grown as monolayers in Dulbecco's Modified Eagle's Medium (DMEM) at 37°C in 5% humidified CO₂. The DMEM was supplemented with 10% Fetal Bovine Serum (FBS), 1% Penicillin-streptomycin (Gibco), 1% Modified Eagle's Medium Non Essential Amino Acids, 1% L-glutamine (Gibco), 1mM sodium pyruvate, 1 µg/ml bovine insulin (Gibco), 1 µg/ml hydrocortisone (Sigma), 1 ng/ml human epithelial growth factor (Gibco) and 1 ng/ml β-estradiol (Sigma).

2.2 Flow cytometry

1 X 10⁶ MCF-7 mp53 cells were harvested by treatment with trypsin and centrifuged at 300 g for 10 minutes at 4°C. The supernatant was removed and the cells were vortexed in 1 ml of 0.5 % formaldehyde in PBS and incubated for 4 minutes at 4°C. Cells were then centrifuged and the supernatant was removed. The cells were resuspended with 1ml of 0.1% of Triton X-100 in PBS for 3 minutes at 4°C, centrifuged and the cell pellet was incubated with 1 ml of 1.0 mg/ml of RNase (Type I-A, Sigma) for

30 minutes at 37°C. The cells were mixed with 1.0 ml of 50 µg/ml propidium iodide, incubated for 30 minutes in the dark at room temperature and filtered through a 48 micron nylon filter. The cells were analyzed on a Coulter EPICS Profile flow cytometer using Cytologic Software (Coulter, Hiatch).

2.3 Drug screening of marine extracts for G2 checkpoint inhibitors

MCF-7 mp53 cells were plated as monolayers at a density of 10,000 cells per well in 96-well polystyrene tissue culture plates (Falcon) in 100 µl of cell culture medium. The cells were allowed to grow for 24 hours and were irradiated with 6.5 Gy of ionizing radiation using a ⁶⁰Co source (Gammacell 200). At 16 hours after irradiation, extracts from marine organisms, stored at about 10 mg/ml in DMSO, were added to the cells at a 1/1000 dilution along with 100 ng/ml of nocodazole (Sigma). Caffeine at 2mM (Sigma, stock 100mM in PBS) was used a positive control. Cells were incubated with the extracts or caffeine for a further 8 hours and then subjected to mitotic ELISA.

2.4 Mitotic ELISA

The medium was carefully removed from a 96-well tissue culture plate with a multi-pipettor and the plate was frozen overnight at -20°C. Cell were thawed by adding 100 µl lysis buffer (1mM EGTA, 0.2 PMSF) to each well. Using a multi-pipettor, the cells were lysed by pipetting up and down 10-15 times and transferring cell lysates to a Nunc-Polysorb 96-well plate. The plate was air dried using a hair dryer at medium setting and placed three feet away. The plate was blocked with 200 µl/well of 5% Carnation dry milk in TBS for one hour at room temperature and then incubated with 100

µl/well of 0.1-0.15 µg/ml TG3 antibody in blocking solution overnight at 4°C. The plate was washed 3 times with washing buffer (10 mM Tris pH 7.4, 0.02% Tween-20) and incubated overnight with HRP-conjugated Goat anti-mouse IgM (Southern Biotechnology Associates) diluted 1/1000 in blocking solution. The plate was washed again and incubated with 120 mM Na₂HPO₄, 100 mM citric acid, pH 4.0, 0.01 % hydrogen peroxide and 0.5 µg/ml ABTS 2,2'-azino-bis(3-ethyl benzthiazalone-6-sulfonic) acid (ABTS, Sigma) for 1 hour at room temperature. The absorbance was measured at 405nm using a 96-well plate reader (Bio-Tek Instruments).

2.5 Mitotic index

Mitotic index values determined by microscopy were adapted from a procedure outlined in Guo *et al* (1995). MCF-7 mp53 cells were plated in 3-cm petri dishes or 6-well plates at a density of 100,000 cells/ml. After being subjected to various treatments, the cells were collected by treatment with trypsin and centrifuged at 300 g for 5 min, washed with 1 ml of PBS and centrifuged again. The cells were suspended in 1 ml of 75 mM KCl for ten minutes at room temperature. After centrifugation, the cells were fixed with 1 ml of methanol: acetic acid, 3:1 for ten minutes at room temperature. The cells were collected by centrifugation as before, and most of the supernatant was removed. The cells were resuspended in the remaining supernatant and transferred to a microscope slide and dried. The slides were stained with 1 µg/ml bis-benzimide (Hoechst No.33258, Sigma) in PBS for 7 minutes at room temperature. Coverslips were mounted on the slides using 90% glycerol in PBS, containing 0.2 M n-propyl gallate and the cells were visualized using a fluorescence microscope. The mitotic index was calculated as:

$$\text{mitotic index} = \frac{\text{\# of cells in mitosis}}{(\text{\# of cells in mitosis} + \text{\# of cells in interphase})} \times 100$$

2.6 Cdc2 immunoprecipitation and kinase assay

Cdc2 immunoprecipitation and kinase assays were performed as described in Gowdy et al (1998) with minor modifications. Treated cells were grown to 70-80% confluence in 10 cm petri dish and subjected to various treatments. The cells were collected by treatment with trypsin and centrifuged and the cell pellet was washed once with 1 mM phenylmethylsulfonyl fluoride (PMSF, Sigma) in PBS. Cells were suspended 20x volume of ice cold lysis buffer (50 mM Tris-HCl, pH 7.4, 150 mM NaCl, 1% NP-40, 1 mM PMSF, 2 µg/ml each of leupeptin, pepstatin and aprotinin, 30 µg/ml DNase I and RNase A, 1 mM dithiothreitol and 1 mM sodium orthovanadate). The cells were lysed by pipetting up and down 20 times, leaving on ice for 15 minutes, pipetting up and down an additional 20 times and leaving on ice for a further 15 minutes. Lysates were cleared by centrifugation at 15,000 xg for 15 minutes. Supernatants were then precleared with rabbit pre-immune serum and 20 µl of washed Protein A Agarose (Gibco BRL) for 30 minutes at 4°C. The cleared lysates were incubated with 1.0 µg of anti-cdc2 antibody for two hours at 4°C, then the lysates were incubated an additional 1 hour with 25 µl of washed protein A agarose. The antigen-antibody complexes were collected by centrifugation and washed five times in lysis buffer.

The immunoprecipitated cdc2 was washed with HI kinase buffer (50 mM Tris-HCl, pH 7.4, 100mM NaCl, 2mM MgCl₂, 1 mM dithiothreitol and 50 µM ATP) three times. The beads were then incubated with 50 µl of H1 kinase buffer along with 1mM sodium orthovanadate, 1µM okadaic acid (Gibco BRL), 0.5 mg/ml histone H1 (Gibco)

and 0.25 mCi/ml [γ - 32 P] ATP (NEN) for 15 minutes at 30°C. The kinase reaction was terminated by boiling samples for 5 minutes in SDS sample buffer and then 20 μ l of samples were resolved on a 15% SDS PAGE gel. The gel was dried and exposed overnight on a Phospho Imager screen. The Cdc2 activity was quantified by measuring intensity of labeled H1 bands using Molecular Dynamic software.

2.7 Western blotting

Cells were lysed in the same manner as for cdc2 immunoprecipitations using the same lysis buffer. Protein concentration was determined using the Biorad Protein Assay. Approximately 50 μ g of protein was resolved by electrophoresis on a 10% SDS-polyacrylamide gel, transferred to a nitrocellulose membrane using a wet transfer apparatus (BioRad) and blocked in 5% Carnation dry milk in TBS-T (10 mM Tris, pH 7.5, 150 mM NaCl, .05% Tween-20) for 1 hour at room temperature. The nitrocellulose membrane was probed with anti-cdc2 antibody (Kinetek) or anti-beta-catenin antibody (Signal Transduction) diluted 1/1000 in blocking solution overnight at 4°C. The nitrocellulose was washed three times for 15 minutes per wash in TBS-T. The membrane was then incubated with either goat anti-mouse IgG (Pierce) or goat anti-rabbit IgG (Gibco) diluted 1/3000 in blocking solution for two hours at room temperature. After washing, the antigen-antibody complexes were visualized by chemoluminescence (SuperSignal, Pierce) and exposed on film (X-OMAT, Kodak).

2.8 Immunofluorescence

MCF-7 mp53 cells were grown overnight in 6-well plates (Falcon) on poly-L-

lysine coated coverslips at a density of 100,000 cells/well. After different treatments, the medium was carefully removed and the coverslips washed once with PBS. The cells were fixed with 3.7% paraformaldehyde in PBS for ten minutes at 4°C. After rinsing cells twice with KB (10 mM Tris, pH 7.5, 150 mM NaCl, 0.1% triton X-100, 0.1% bovine serum albumin), the coverslips were incubated with primary antibody diluted in KB for 1.5 hours at room temperature. The following primary antibody is diluted 1/100: Cyclin A (Santa Cruz), Cyclin B (Santa Cruz), Cdk2, cdc25B (Transduction Laboratories), cdc25C (Santa Cruz), 14-3-3 β (Santa Cruz), GSK-3 β (Transduction Laboratories), β -catenin (Transduction Laboratories) and Wee1 (Kinetek). The anti-p34^{cdc2} antibody from Kinetek was diluted 1/400. The coverslips were washed twice with KB for ten minutes each wash. Next the coverslips were incubated 1.5 hours at room temperature with either Cy3-conjugated anti-mouse or anti-rabbit secondary antibody at a dilution of 1/750 in KB and washed twice again in KB. The DNA was stained by immersing coverslips in 0.1 μ g/ml of bis-benzimide and washed once more with KB. The coverslips were mounted on microscope slides using 90% glycerol in PBS using 0.2M n-propyl gallate. The cells were observed using a Zeiss Axiophot fluorescence microscope and photographs taken using Kodak Tmax 400 film.

2.9 Preparation of nuclear extract

MCF-7 mp53 cells subjected to various treatment were collected by trypsinization and centrifugation and washed with PBS. The cell pellets were suspended in 20 volumes of lysis buffer (10 mM Tris, pH 6.8, 1 mM CaCl₂, 1.5 mM MgCl₂, 0.2 PMSF, 250 mM Sucrose, 0.5% Triton X-100) and allowed to swell on ice for 10 minutes. The cells were

homogenized using a tight-fitting dounce homogenizer and nuclei collected by centrifugation at 500xg for 5 minutes. The nuclei were washed three times with isolation buffer (lysis buffer without Triton X-100), resuspended in 20 vol of isolation buffer and lysed by boiling in 4X SDS sample buffer. The extracts were ran on a 10% SDS Page gel and stained with Coomassie Blue to ensure equal protein loading for western blots.

2.10 Production and purification of recombinant GSK-3 β

The procedure is adapted from the Sadowski laboratory (Dept. Biochemistry and Molecular Biology, UBC) and contains some modifications. A preculture of an *E. coli* BL-21 strain overexpressing wildtype GSK-3 β with a GST tag was grown overnight in LB medium supplemented with 100 μ g/ml ampicillin (Sigma). The overnight culture was diluted 1/100 in LB medium with ampicillin and grown for 2 hours. The expression of GSK-3 β was induced by the addition of 1mM IPTG to culture medium for an additional 2 hours. The cells were harvested by centrifugation at 5000 xg for 10 minutes and suspended in 20 vol of lysis buffer (50mM NaCl, 50 mM Tris- pH 7.5, 5mM EDTA, 1 μ g/ml leupeptin, 1 μ g/ml pepstatin and 150 μ M PMSF). The cells were subjected to three cycles of sonication of 1 minute each and left on ice for five minutes in between sonications. The cellular debris was pelleted out by centrifugation at 10, 000 xg for 10 minutes.

A 1:1 slurry of glutathione-agarose was prepared by hydrating 40 mg of dried glutathione-agarose (Sigma, G-4510) with 600 μ l of distilled H₂O for one hour at room temperature and washed three times in lysis buffer. The agarose beads were pelleted by centrifugation at 2000 rpm for two minutes. The bacterial cell lysates were incubated

with 10% volume of the glutathione-agarose slurry on a nutator for one hour at 4°C. The glutathione agarose was washed three times with 20 vol of lysis buffer. The GST tagged GSK-3 β was eluted by incubation of the beads in 250 μ l of elution buffer (5mM glutathione, 2mM DTT in lysis buffer) on a nutator for one hour at 4°C. A sample of each purification step was boiled with SDS sample buffer and run onto a 10% SDS PAGE gel to monitor the purification of the GSK-3 β kinase.

2.11 GSK-3 β phosphotransferase assay

The GSK-3 β kinase assay was adapted from a procedure used by Kinetek Pharmaceuticals with some modifications. Approximately 5 μ g of purified recombinant GSK-3 β was diluted in 35 μ l of GSK-3 β Reaction Buffer (8mM MOPS, pH 6.8, 0.2 mM EDTA and 10 mM magnesium acetate). To initiate kinase reactions, 4 μ g GSK-3 β peptide substrate [YRRAAVPPSPSLSRHSSPHQS(PO₃H₂)EDEEE] and 5 μ Ci of [γ -³²P]ATP (NEN) were added. After incubation in a 30°C water bath for 20 minutes, 15 μ l of the reaction buffer was spotted onto P81 cation exchanger chromatography paper disks (Whatman) with a diameter of 2.5 cm. The chromatography papers were dried and then washed five times with 1% phosphoric acid for five minutes each wash. The washed filter papers were then transferred to numbered scintillation vials with 2 ml of scintillation fluid and radioactivity was counted with a Beckman Scintillation Counter. The cpm values were converted to a rate of activity corresponding to pmol PO₄ incorporated/(nmol peptide x min).

Chapter 3

Results

Identification of G2 Checkpoint Inhibitors debromohymenialdisine and isogranulatimide

3.1 Initial screen of 1300 marine extracts

To identify novel G2 checkpoint inhibitors, a high-throughput assay was developed in our laboratory (Roberge et al, 1998). I used this assay to screen 1500 marine extracts for G2 checkpoint inhibitors. Briefly, MCF-7 mp53 cells grown in 96-well plates were irradiated with 6.5 Gy of ionizing radiation. At 16 hours after irradiation the cells were arrested in G2 (figure 9). Diluted marine extracts were then added along with nocodazole and the cells were incubated for an additional 8 hours. A mitotic ELISA assay was then performed on these cells to identify extracts containing G2 checkpoint inhibitors i.e. that permit the G2-arrested cells to enter mitosis. From this initial screen, four marine extracts were found to contain activity. In a collaborative effort with Dr. Raymond Andersen's laboratory in the Department of Oceanography and Organic Chemistry at U.B.C., these extracts were subjected to assay-guided fractionation to purify the active components and their chemical structures were elucidated.

In general, the purification scheme in isolating the compound of interest began

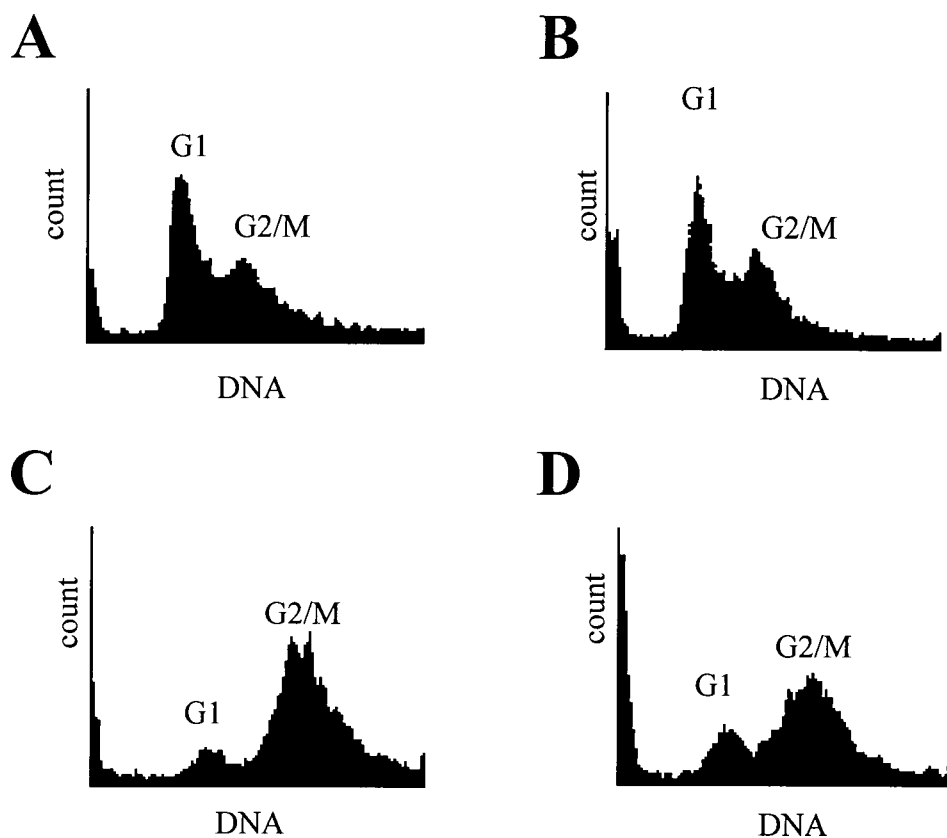


Figure 9. Cell cycle profile of G2 arrest in MCF-7 mp53 cells

MCF-7 mp53 cells were mock-irradiated (A) or irradiated with 6.5 Gy of ionizing radiation and collected 8 (B), 16 (C) and 24 (D) hours later. The cells were fixed in 0.5% formaldehyde in PBS, incubated with RNase 1, stained with propidium iodide and subjected to flow cytometry. The y-axis is the cell count and x-axis is the DNA content. The peaks represent cells that are either in G1 phase or G2/M phase.

with the suspension of the crude extract in water and extraction with hexanes, dichloromethane and ethyl acetate. The fractions containing activity were identified using the assay described above and were separated using Sephadex LH20 chromatography followed by HPLC, centrifugal thin layer chromatography, counter current chromatography, or open column chromatography. The structures of the compounds were elucidated using 1D and 2D NMR techniques and molecular mass was determined by mass spectroscopy.

The first G2 checkpoint inhibitors identified by Bruno Cinel were debromohymenialdisine and its derivative bromohymenialdisine (figure 10A), which were isolated from the sponge *Styllessa flabelliformis* collected in the waters of Papua New Guinea. A second positive extract was found by Lin Xu to contain staurosporine-a known G2 checkpoint inhibitor (Tam and Schlegel, 1992; figure 10B) and its oxazolidine derivative (figure 10C). Finding staurosporine was encouraging as it validated the ability of the assay to identify G2 checkpoint inhibitors. A third extract, from the ascidian, *Didemnum granulatum* collected off the coast of Brazil, was shown by Dr. Roberto Berlinck to contain a structurally novel G2 checkpoint inhibitor, isogranulatimide (figure 10D, Roberge *et al.*, 1998, Berlinck *et al.*, 1998). My research focused on the two novel checkpoint inhibitors debromohymenialdisine and isogranulatimide.

3.2 Activity profiles of debromohymenialdisine and isogranulatimide

Debromohymenialdisine and isogranulatimide were added at different concentrations along with nocodazole to G2-arrested MCF-7 mp53 cells for 8 hours. The relative proportion of cells in mitosis was then determined either as the absorbance

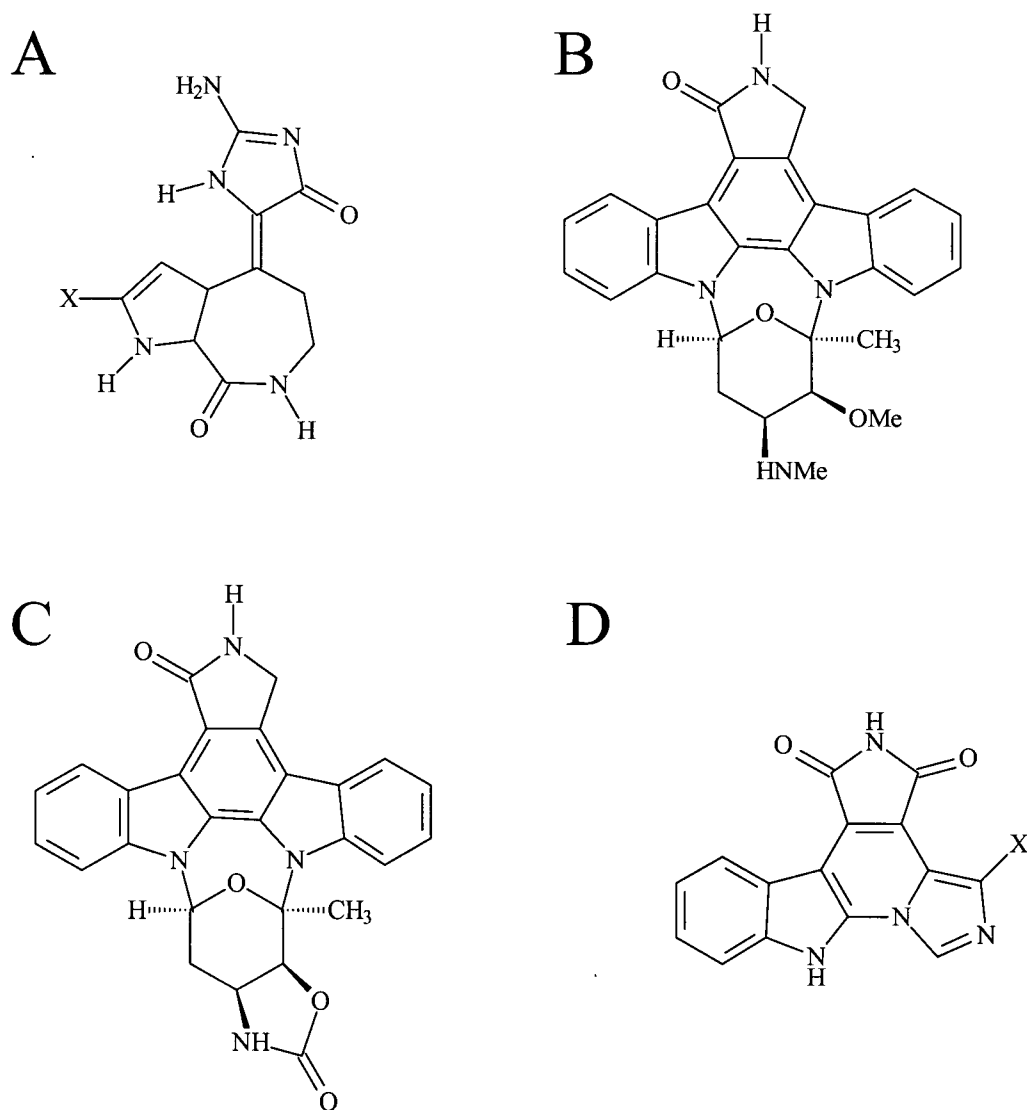


Figure 10. Structures of G2 checkpoint inhibitors isolated from marine extracts

A: Hymenialdisine (X=Br), debromohymenialdisine (X=H); B: staurosporine; C: oxazolidone derivative of staurosporine; D: isogranulatimide, X denotes site of radioiodination

reading obtained by mitotic ELISA assay or as the mitotic index obtained by microscopy. Using the results of the ELISA, the concentration giving half-maximal inhibitory activity (IC_{50}) of debromohymenialdisine and isogranulatimide (figure 11A and B) were 10 μ M and 2 μ M, respectively. The IC_{50} values obtained by microscopy (figure 11C and D) were 10 μ M for debromohymenialdisine and 8 μ M for isogranulatimide. Results from both the mitotic ELISA and mitotic index determination showed maximal activity at 40 μ M for debromohymenialdisine and at 20 μ M for isogranulatimide. At concentrations greater than the maximal, the activity decreased due to drug toxicity for both compounds as was observed visually by the appearance of apoptotic nuclei.

Investigation of the mechanism of action of debromohymenialdisine and isogranulatimide

3.3 Effects of debromohymenialdisine and isogranulatimide on Cdc2 kinase

To elucidate the mechanism by which debromohymenialdisine and isogranulatimide overcame G2 arrest, I examined the effect of these inhibitors on a key regulator of entry into mitosis, Cdc2 kinase. When cells are arrested in G2, the p34^{cdc2} subunit of Cdc2 kinase is inhibited by phosphorylation at its Thr14 and Tyr15 residues by the kinases Myt1 and Wee1 respectively (Liu *et al.*, 1997, McGowan and Russell, 1995). In order for cells to enter mitosis, p34^{cdc2} must be dephosphorylated at these sites by cdc25C to initiate downstream events of mitosis. However, it has been shown that cells treated with okadaic acid or fostreicin may be induced to enter mitosis independently of Cdc2, suggesting they may act on a pathway independent of Cdc2 or act downstream of

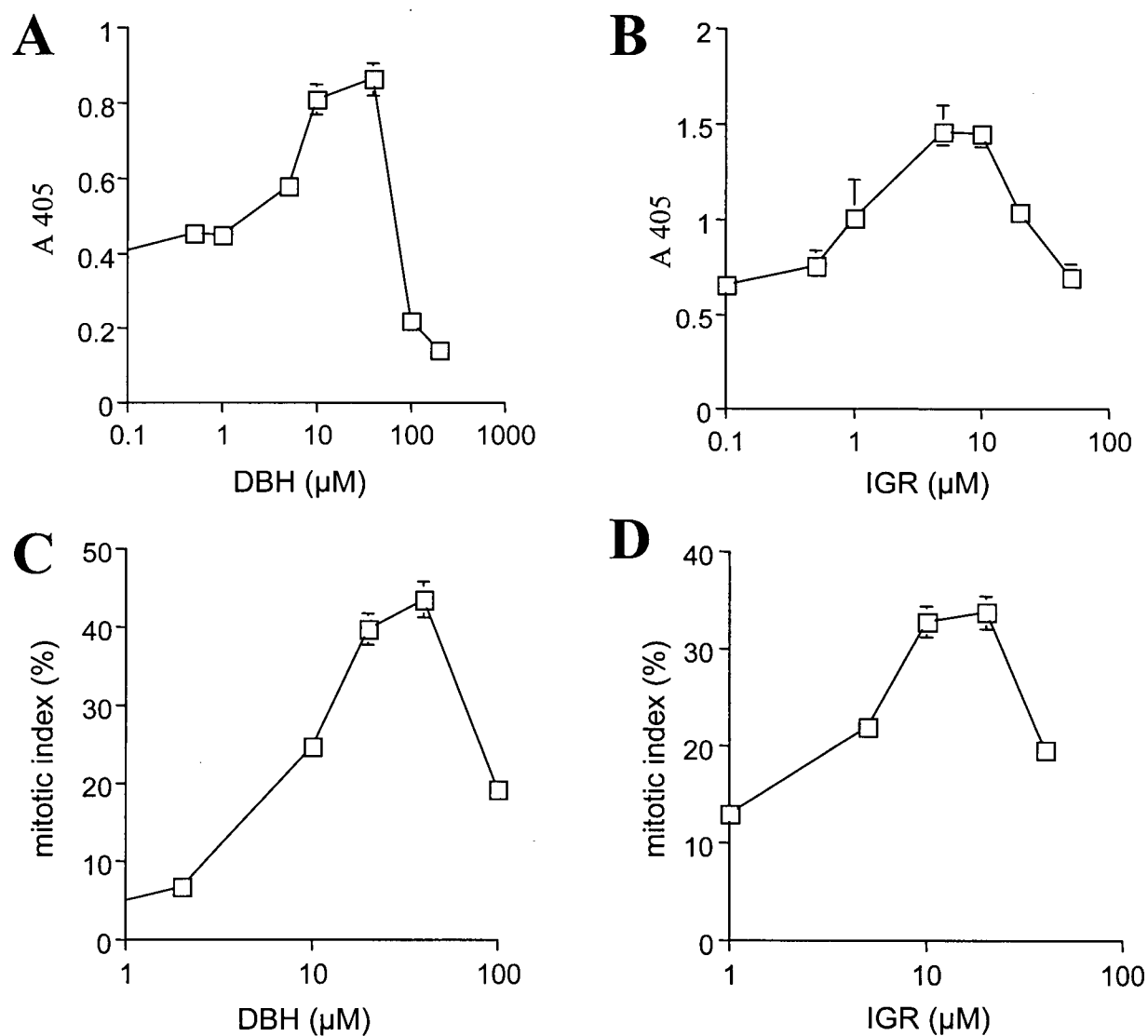


Figure 11. G2 checkpoint inhibition profile of debromohymenialdisine and isogranulatimide

MCF-7 mp53 cells plated in 96-well plates (A, B) or six-well plates (C, D) were exposed to 6.5 Gy of ionizing radiation. 16 hours later, debromohymenialdisine (DBH) or isogranulatimide (IGR) were added at the indicated concentrations along with nocodazole for an additional 8 hours. The cells were either subjected to the mitotic ELISA (A, B) or stained with Hoechst 33258 and their mitotic index determined by microscopy (C, D).

Cdc2 (Gowdy *et al.*, 1998). Therefore, I determined whether debromohymenialdisine and isogranulatimide are inducing entry into mitosis that is dependent on p34^{cdc2} dephosphorylation and Cdc2 activation.

3.3a Debromohymenialdisine and isogranulatimide stimulate the dephosphorylation of Cdc2

The phosphorylation states of p34^{cdc2} affect its mobility in SDS-PAGE and may be visualized as three bands in western blots (Mueller *et al.*, 1995). The slowest moving band is the doubly phosphorylated protein, the intermediate band is the singly phosphorylated protein and the faster migrating band is hypophosphorylated. Debromohymenialdisine (40µM) and isogranulatimide (10µM) were added to MCF-7 mp53 cells 16 hours after irradiation with 6.5 Gy. The cells were harvested after incubation with the drugs for 2, 4 or 6 hours and they were lysed. The protein concentration was determined and the proteins were denatured in SDS sample buffer. Protein (25 µg) was resolved with a 10% SDS-PAGE gel, transferred onto nitrocellulose and a western blot was performed using an antibody that recognizes p34^{cdc2} (Kinetek). Three bands corresponding to these three forms were present in G2-arrested cells (figure 12). Cells arrested in mitosis using the antimicrotubule agent nocodazole showed a disappearance of the upper bands and an increase in the intensity of the lower band, indicating dephosphorylation of p34^{cdc2}. Treatment with nocodazole for 16 hours blocked ~60% of the cells in mitosis. This indicates that inhibitory phosphorylation contributes to G2 arrest in γ-irradiated MCF-7 mp53 cells.

Cells arrested in G2 that were incubated with debromohymenialdisine and isogranulatimide for 2, 4 and 6 hours show time-dependent dephosphorylation of p34^{cdc2}

(figure 12). Caffeine and UCN-01 were included for comparison in this experiment as they are known G2 checkpoint inhibitors. They also caused the dephosphorylation of p34^{cdc2} at a rate similar to debromohymenialdisine and isogranulatimide.

3.3b Debromohymenialdisine and Isogranulatimide cause an increase in Cdc2 kinase activity

To determine the effect of the checkpoint inhibitors on Cdc2 kinase activity, MCF-7 mp53 cells were treated with checkpoint inhibitors for seven hours and then the cells were collected and lysed in H1 kinase lysis buffer. Cdc2 kinase was immunoprecipitated with anti-p34^{cdc2} antibody and its kinase activity was measured by its ability to phosphorylate histone H1 with [γ -³²P] ATP. The labeled histone was resolved on a 10% SDS-PAGE gel, which was dried and exposed on a Phosphor Imager screen.

Figure 13 shows there was little or no Cdc2 kinase activity in irradiated G2-arrested cells but there was strong activity in mitotic cells, in which p34^{cdc2} is dephosphorylated. The G2 checkpoint inhibitors all caused activation of the Cdc2 kinase. The novel G2 checkpoint inhibitors debromohymenialdisine at 40 μ M and isogranulatimide at 10 μ M caused a five-fold activation of Cdc2 kinase as compared to G2-arrested cells (figure 13). UCN-01 (20 nM) and caffeine (2mM) also activated the Cdc2 kinase to the same degree. However, there was a decrease in Cdc2 kinase activity when cells were treated with 60 nM of UCN-01 because at this concentration the drug exhibits toxicity. Taken together, the results on p34^{cdc2} phosphorylation and Cdc2 kinase activity show that debromohymenialdisine and isogranulatimide overcame G2 arrest by overcoming the inhibitory phosphorylation that normally inactivates Cdc2 kinase in G2-arrested cells. Although the checkpoint inhibitors may have several targets, at least one

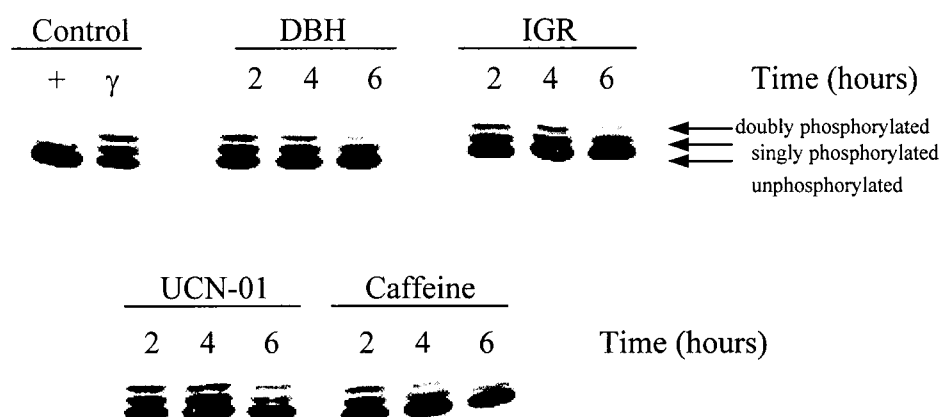


Figure 12. Effect of G2 checkpoint inhibitors on the phosphorylation of p34^{cdc2}

MCF-7 mp53 cells arrested at G2 were treated with 40 μ M debromohymenialdisine (DBH) or 10 μ M isogranulatimide (IGR) for 2, 4 and 6 hours. The controls were mitotic cells obtained by treating cells for 20 hours with nocodazole (+) and G2-arrested cells collected at 16 hours after irradiation with 6.5 Gy (γ). Western blots were performed using anti-p34^{cdc2} antibody. The three phosphorylation states are indicated as arrows corresponding to doubly phosphorylated, singly phosphorylated and unphosphorylated p34^{cdc2}.

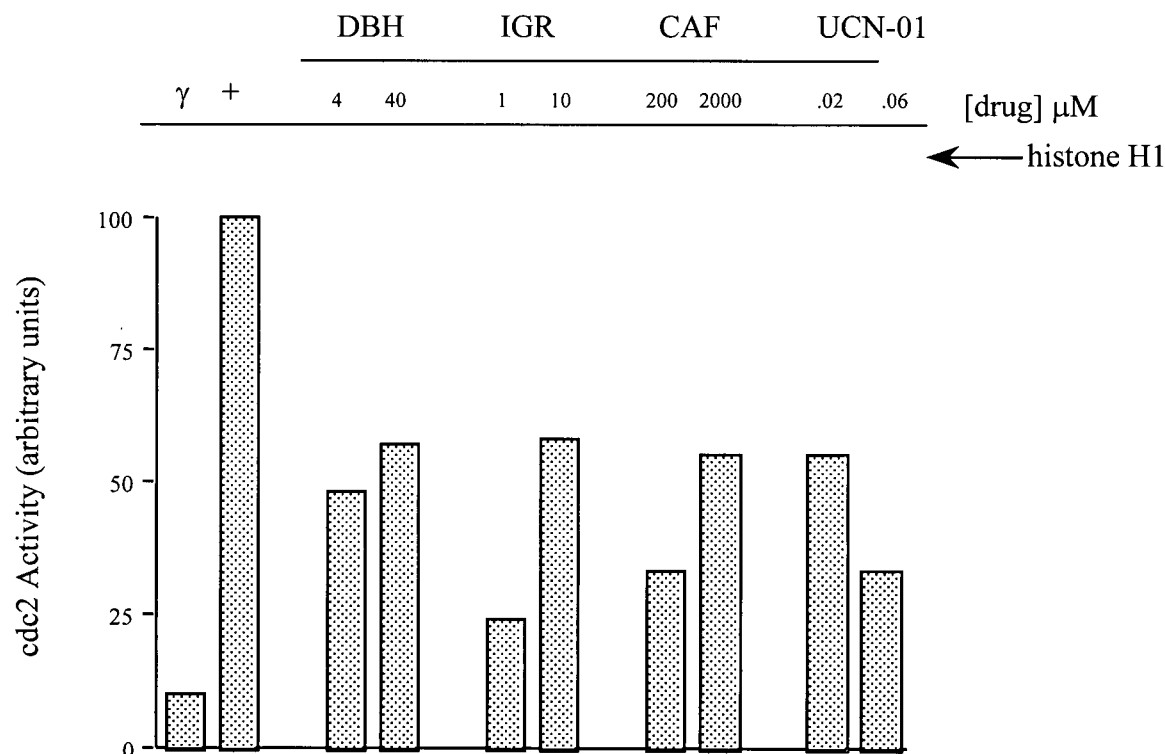


Figure 13. Cdc2 kinase activity in response to checkpoint inhibitors

Activity of Cdc2 kinase in response to the checkpoint inhibitors was measured by H1 kinase assay. Cells arrested in G2 were treated with two different concentrations of the G2 checkpoint inhibitors debromohymenialdisine (DBH), isogranulatimide (IGR), UCN-01 and caffeine (CAF) for 6 hours. Cdc2 kinase was immunoprecipitated from the cells and kinase activity assayed with $[\gamma\text{-}^{32}\text{P}]\text{ATP}$ using histone H1 as the substrate for cdc2. Also included were cells arrested in G2 (γ) and mitotic cells (+).

The intensity of radiolabelled histone H1 (indicated by arrow) was quantified by Molecular Dynamics software. Relative Cdc2 kinase activity is represented in the bar graph using arbitrary units.

target must act upstream of the Cdc2 kinase. My subsequent research involved many approaches to try to identify these targets.

3.4 Inhibition of the activity of debromohymenialdisine and isogranulatimide by phenylarsine oxide

Dephosphorylation of the inhibitory Thr14 and Tyr15 residues on p34^{cdc2} is normally carried out by the protein phosphatase cdc25C. It is possible that the G2 checkpoint inhibitors activate the Cdc2 kinase by activating cdc25C. Protein tyrosine phosphatases contain vicinal thiols in their active site and are inhibited by compounds such as phenylarsine oxide, which bind covalently to adjacent thiols. Cells arrested in G2 were treated with different concentrations of phenylarsine oxide for 15 minutes. Debromohymenialdisine and isogranulatimide were added for 6 hours and G2 checkpoint inhibition was determined by microscopy.

Figure 14 shows phenylarsine oxide prevented debromohymenialdisine and isogranulatimide from overcoming the G2 checkpoint. Half-maximal inhibition was observed at about 0.1 μ M phenylarsine oxide and 6 μ M caused complete inhibition. This strongly suggests that the activity of the checkpoint inhibitors requires the activity of a tyrosine phosphatase, very possibly cdc25B or C.

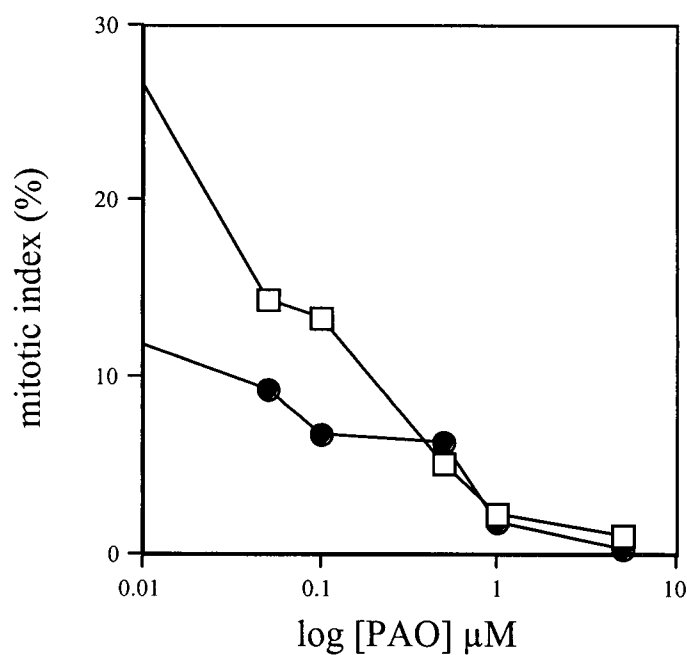


Figure 14. Inhibition of debromohymenialdisine and isogranulatimide by phenylarsine oxide

MCF-7 mp53 cells were arrested in G2 by exposure to 6.5 grays of irradiation and were treated with different concentrations of phenylarsine oxide (PAO) for 15 minutes. After removal of phenylarsine oxide, the cells were treated with debromohymenialdisine (40 μM , \square) or isogranulatimide (10 μM , \bullet) for 6 hours along with nocodazole. The mitotic index was then determined by microscopy.

3.5 Identifying the in vivo targets of debromohymenialdisine and isogranulatimide

3.5a Coupling debromohymenialdisine to a solid support

I attempted to identify the direct target of these checkpoint inhibitors using affinity chromatography. Debromohymenialdisine contains a primary amine (figure 9A) which may be coupled to epoxy-activated agarose beads. It was hoped that incubating the debromohymenialdisine-agarose with cell extracts would allow us to purify and identify its target protein. Preliminary experiments involved incubating debromohymenialdisine-agarose or agarose with lysates collected from cells that were arrested in G2 16 hours after irradiation. After washing, the bound proteins were eluted from the agarose by adding SDS sample buffer and were then separated by SDS-PAGE and visualized by silver staining. No protein bands were found that interacted specifically with the debromohymenialdisine-agarose and not with agarose; all bands associated with the debromohymenialdisine-agarose beads were also associated with the agarose beads alone.

3.5b Radiolabeling of isogranulatimide with ¹²⁵Iodine

Examination of the structure of isogranulatimide (figure 9D) suggested that it could be radiolabeled by reaction with iodine in the presence of trifluoroacetic acid. The radiolabeled compound could then be used to detect the target protein by performing overlay assays. The procedure involves the incubation of the drug with a SDS-gel or nitrocellulose membrane in which cell extracts have been resolved by electrophoresis. Exposure of either the membrane or gel to film may reveal radiolabeled protein bands

that have interacted with ^{125}I -isogranulatimide.

First, the activity of purified iodogranulatimide, prepared by Robert Britton, was tested using the G2 checkpoint inhibition assay. Its activity was three-fold diminished when compared to isogranulatimide (not shown) but was considered sufficiently high to proceed further. ^{125}I -isogranulatimide was prepared and used in overlay assays to try to detect interacting proteins. I separated by SDS-PAGE extracts of MCF-7 mp53 cells that were mock-irradiated or irradiated and harvested 1, 2, 5, 8, 16 or 24 hours after irradiation. The resolved proteins were either transferred onto a nitrocellulose membrane or the gel itself was washed, the proteins denatured with guanidium hydrochloride and then were renatured in the presence of β -mercaptoethanol. The membrane or gel was incubated with ^{125}I -isogranulatimide and exposed to film. No bands were detected on the nitrocellulose membrane (not shown). Some labeled protein bands were detected on the gels (not shown). However, the bands corresponded to proteins that were very abundant, which suggests that the interactions were non-specific in nature.

3.6 Effects of checkpoint inhibitors on the abundance and subcellular localization of cell cycle regulatory proteins

The cell cycle is regulated not only by the changes in activity of cyclin-dependant kinases and phosphatases but also by changes in their abundance or their intracellular distribution. For example, cyclin B accumulates in the cytoplasm during G2 phase and associates with p34^{cdc2} , whose abundance changes through the cell cycle. p34^{cdc2} is dependent upon its association with cyclin B to be active as the Cdc2 kinase. At the

onset of mitosis, cyclin B becomes rapidly translocated to the nucleus presumably to initiate the events of mitosis such as nuclear envelope breakdown (Jin *et al.*, 1998).

To further study the mechanism of action of debromohymenialdisine and isogranulatimide, I examined their effects on the distribution and abundance of a wide variety of cell cycle regulators that have been implicated in either G2 arrest or in the G2-M phase transition. I studied their distribution and abundance by immunocytochemistry using antibodies that are specific for each cell cycle regulator. MCF-7 mp53 cells were grown overnight on poly-L-lysine coated coverslips and irradiated with 6.5 Gy of ionizing radiation. Sixteen hours later when the cells are arrested in G2, debromohymenialdisine and isogranulatimide were added. The coverslips were processed for immunofluorescence three hours later. In addition, two known G2 checkpoint inhibitors, caffeine and UCN-01 were also used. The controls used were unirradiated cells or cells irradiated and harvested after 16 hours or 19 hours without exposure to G2 checkpoint inhibitors. The coverslips were incubated with the primary antibody and with Cy3- conjugated antibody to detect the protein and were treated with Hoechst 33258 to stain the DNA to determine the cell cycle stage. Some cells were treated with secondary antibody alone and in all cases showed no significant fluorescence. The preparations were viewed with a Zeiss Axiophot fluorescence microscope and photographed using Kodak TMAx 400 film. The photographs were examined if irradiation or the addition of checkpoint inhibitors caused a change in intracellular compartmentalization of the protein or caused a change in the intensity of the fluorescence signal.

3.6a Cyclin A

I first examined cyclin A, which associates with Cdk2 to form an active complex that controls the progression of the cell through S-phase. However, some evidence suggests that cyclin A/Cdk2 may also play a role in G2-M phase transition (Pagano *et al.*, 1992). Immunofluorescence showed that in mock-irradiated interphase cells, cyclin A was concentrated in the nucleus with large speckles found in the cytoplasm (figure 15A). Neither irradiation nor treatment with G2 checkpoint inhibitors caused any change in the subcellular organization or abundance of cyclin A (figure 15C-L).

3.6b Cyclin B

Cyclin B1 associates with p34^{cdc2} to form Cdc2 kinase which, when dephosphorylated by cdc25C at Thr14 and Tyr15, becomes activated and initiates the events of mitosis. In mock-irradiated interphase cells, cyclin B1 was found throughout the cytoplasm with a noticeable accumulation in a ring around the nucleus (figure 16A). This suggests that cyclin B1 was being actively excluded from the nucleus. Irradiation caused no change in the subcellular organization of cyclin B1 (figure 16C-E). Cells treated with the G2 checkpoint inhibitors but still remaining in interphase also showed no change (figure 16H-P). However cells treated with G2 checkpoint inhibitors that were now in prophase were observed to have a nuclear accumulation of cyclin B (as indicated by arrows in figure 16 I, K, M and O). Since nuclear accumulation of cyclin B1 occurs at or just before the onset of mitosis (Jin *et al.*, 1998), this indicates that the G2 checkpoint inhibitors tested are acting upstream of cyclinB/cdc2 causing a normal entry into mitosis.

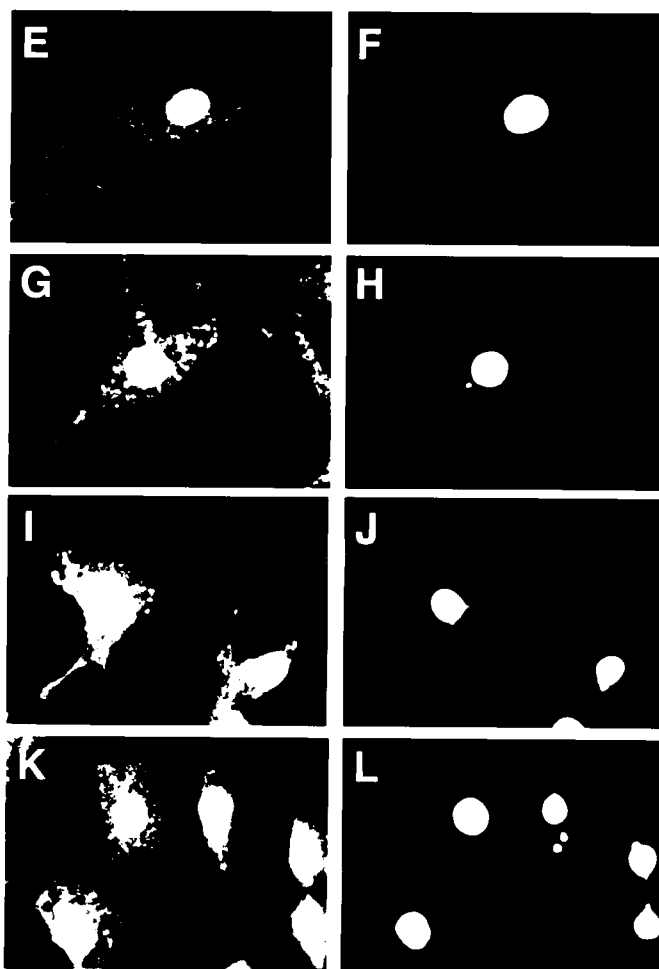
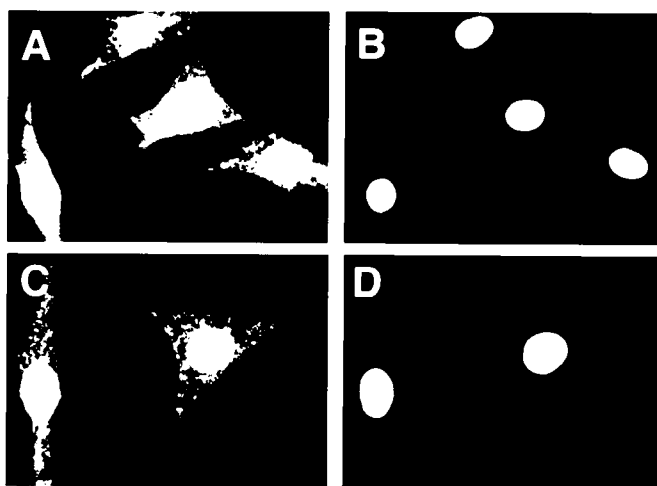


Figure 15. Nuclear/cytoplasmic distribution of cyclin A

MCF-7 mp53 cells were mock irradiated (A, B) or irradiated with 6.5 Gy and observed 19 hours later (C, D) or irradiated and 16 hours later treated for three hours with 40 μ M debromohymenialdisine (E, F), 10 μ M isogranulatimide (G, H), 10 nM UCN-01 (I, J) and 2mM caffeine (K, L). Rows are matched photographs of cells showing cyclin A immunofluorescence to the left and DNA stain to the right.

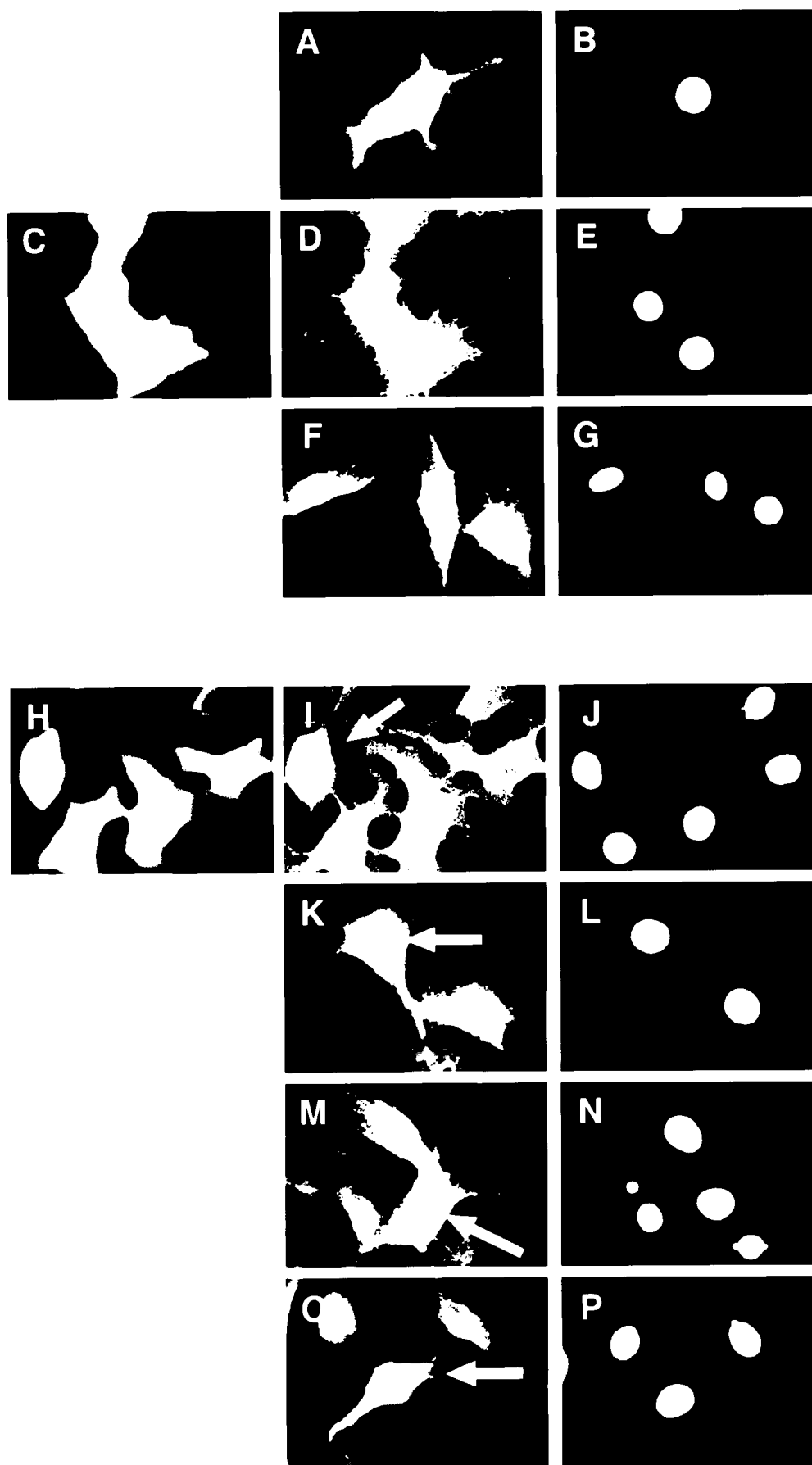


Figure 16. Nuclear/cytoplasmic distribution of cyclin B1

MCF-7 mp53 cells were mock irradiated (A, B), irradiated with 6.5 Gy and observed 16 hours (C, D, E) and 19 hours later (F, G) or 16 hours later treated for three hours with 40 μ M debromohymenialdisine (H, I, J), 10 μ M isogranulatimide (K, L), 10 nM UCN-01 (M, N) and 2mM caffeine (O, P). Cells indicated by arrows are in prophase. Rows are matched photographs of cells showing cyclin B1 immunofluorescence to the left and DNA stain to the right.

3.6c Cyclin-dependent kinases: p33^{cdk2} and p34^{cdc2}

Cdk2 is believed to control entry into mitosis by mediating the activation of cdc2 (Guadagno and Newport, 1996). In mock irradiated cells, Cdk2 was found to be almost exclusively nuclear with very fine speckles in the cytoplasm (figure 17A). The intensity and localization of cdk2 was not altered by irradiation (figure 17C) or treatment with G2 checkpoint inhibitors (figure 17E-K). On the other hand, Cdc2 was found to be evenly dispersed throughout the cytoplasm and the nucleus of both unirradiated interphase cells (figure 18A) and irradiated cells (figure 18 C-F). However, addition of debromohymenialdisine caused an increase in signal intensity of cdc2 in or around the nucleus (figure 18G and H) that was not evident with the addition of the other G2 checkpoint inhibitors (figure 18K-P).

3.6d Phosphatases: cdc25B and cdc25C

Cdc25B and cdc25C are cdk phosphatases involved in the G2-M phase transition (Lammer *et al.*, 1998). Cdc25B was found to be mainly nuclear with fine cytoplasmic staining showing no change after irradiation (figure 19A) or addition of drugs (figure 19C-E). In mock-irradiated interphase cells, cdc25C was very evenly dispersed throughout the cytoplasm and nucleus (figure 20A). However, irradiation caused a concentration of cdc25C to appear as a ring around the nucleus (figure 20C). It appears that cdc25C was either being excluded from the nucleus or was being prevented from entering the nucleus (figure 20C). Debromohymenialdisine also appeared to cause an increase in cdc25C signal (figure 20G), as was the case for cdc2 (figure 17G). This increase in signal was not observed in cells treated with the other checkpoint inhibitors.

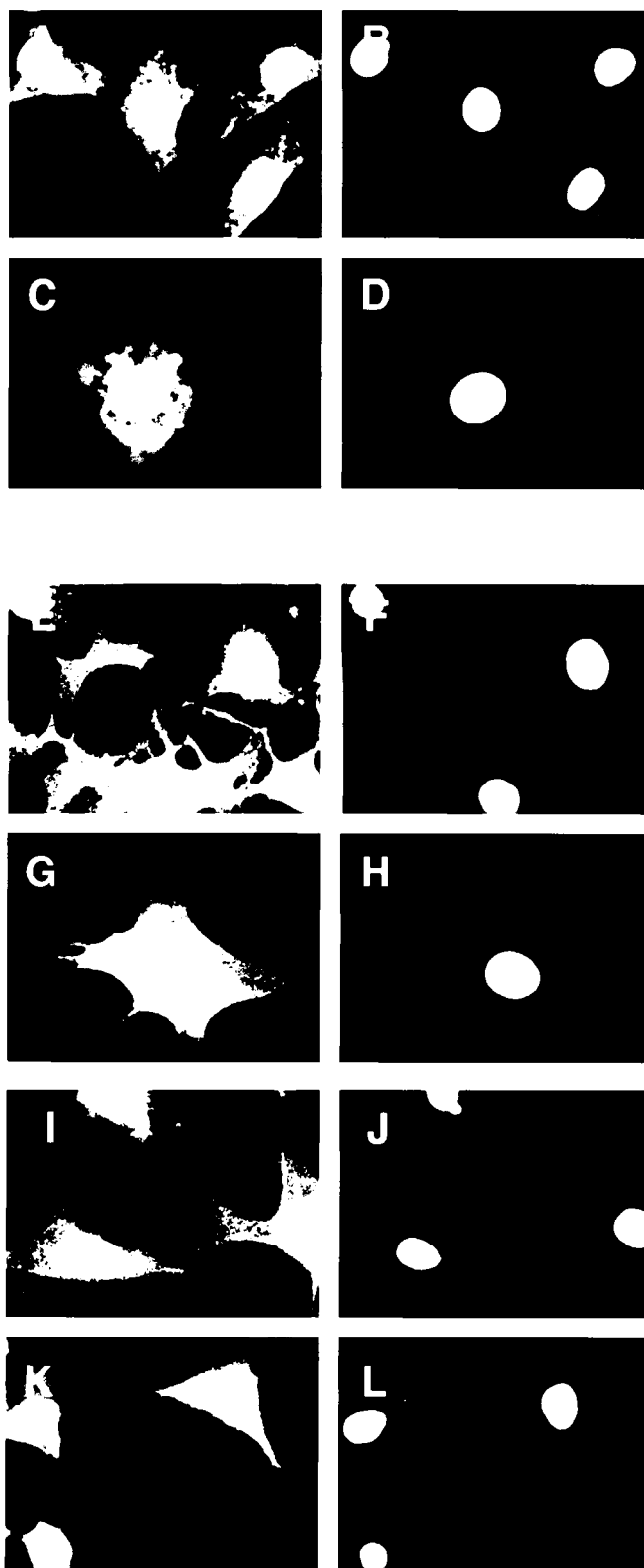


Figure 17. Nuclear/cytoplasmic distribution of Cdk2

MCF-7 mp53 cells were mock-irradiated (A, B), irradiated with 6.5 Gy and observed 19 hours later (C, D), or 16 hours after irradiation treated for three hours with 40 μ M debromohymenialdisine (E, F), 10 μ M isogranulatimide (G, H), 10 nM UCN-01 (I, J) and 2 mM caffeine (K, L). Rows are matched photographs of cells showing Cdk2 immunofluorescence to the left and DNA stain to the right.

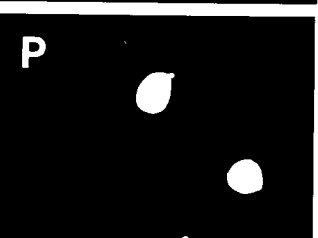
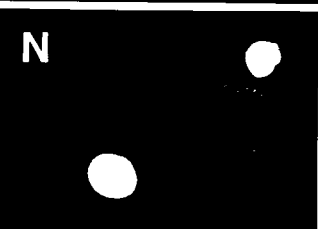
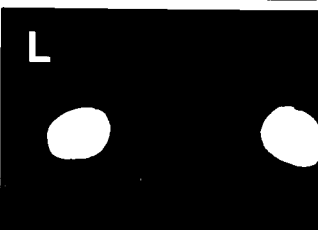
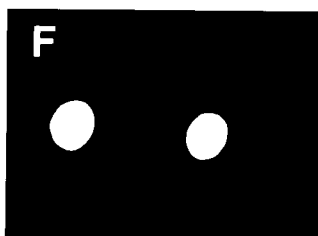
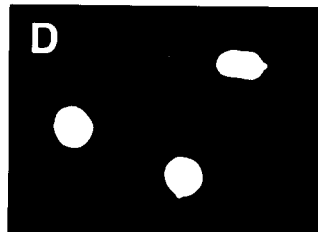
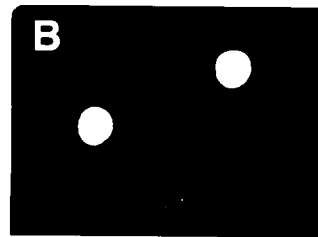


Figure 18. Nuclear/cytoplasmic distribution of Cdc2

MCF-7 mp53 cells were mock-irradiated (A, B), irradiated with 6.5 Gy and observed 16 (C, D) or 19 hours later (E, F) and 16 hours after irradiation treated for three hours with 40 μ M debromohymenialdisine (G, H, I), 10 μ M isogranulatimide (K, L), 10 nM UCN-01 (M, N) and 2 mM caffeine (O, P). Rows are matched photographs of cells showing Cdc2 immunofluorescence to the left and DNA stain to the right. All photos were taken at an exposure time of 15 seconds except for photo G which is a 5 second exposure.

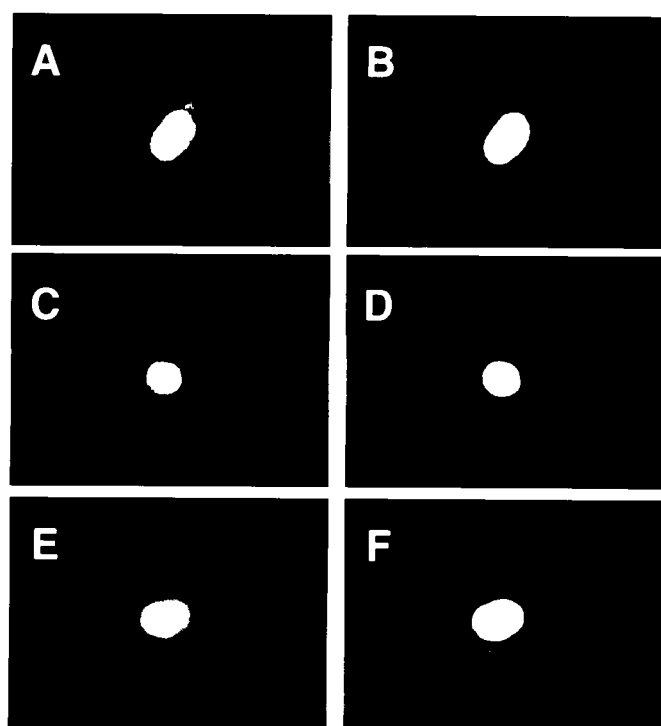


Figure 19. Nuclear/cytoplasmic distribution of cdc25B

MCF-7 mp53 cells were irradiated with 6.5 Gy and observed 19 hours later (A, B), and treated for three hours with 40 μ M debromohymenialdisine (C, D) and 10 μ M isogranulatimide (E, F). Rows are matched photographs of cells showing cdc25B immunofluorescence to the left and DNA stain to the right.

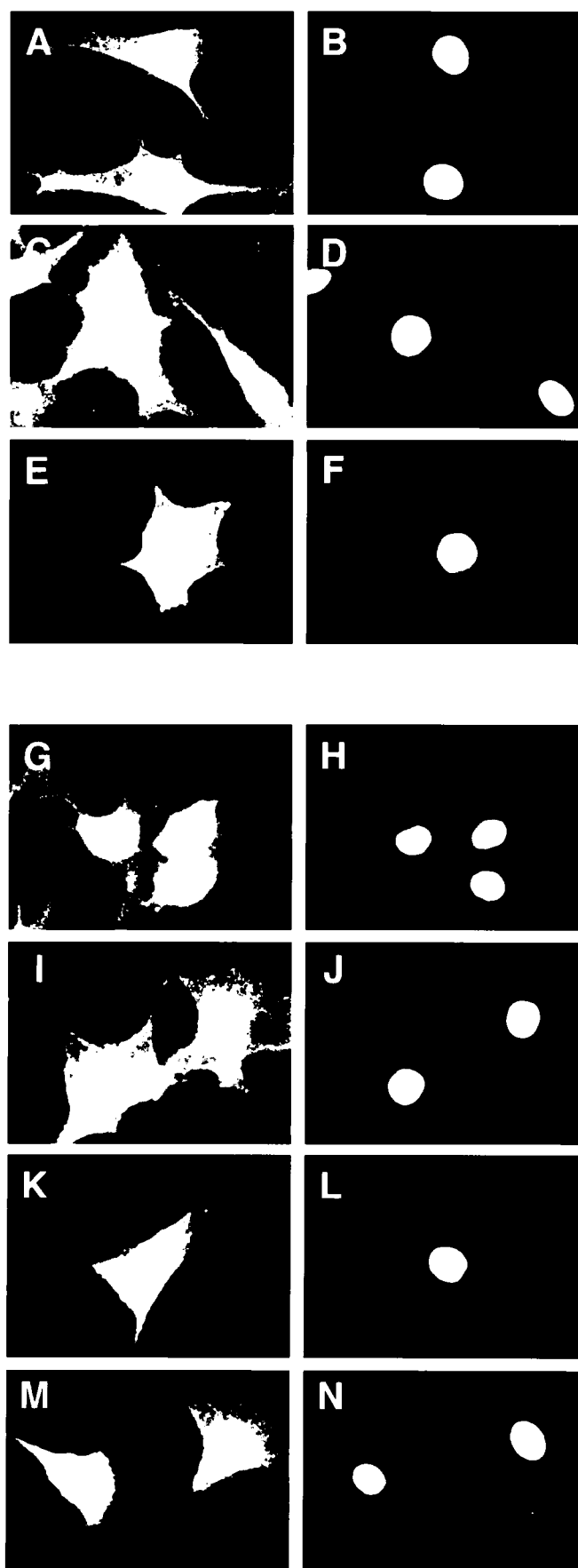


Figure 20. Nuclear/cytoplasmic distribution of cdc25C

MCF-7 mp53 cells were mock irradiated (A, B), irradiated with 6.5 Gy and observed 16 hours (C, D) and 19 hours later (E, F) or 16 hours later treated for three hours with 40 μ M debromohymenialdisine (G, H), 10 μ M isogranulatimide (I, J), 10 nM UCN-01 (K, L) and 2mM caffeine (M, N). Rows are matched photographs of cells showing cdc25C immunofluorescence to the left and DNA stain to the right.

3.6e Wee1

Wee1 is the kinase that phosphorylates p34^{cdc2} at Tyr 15 causing inhibition of the Cdc2 kinase (McGowan and Russell, 1993). Wee1 in mock-irradiated cells was shown to be nuclear, with fine speckles in the cytoplasm (figure 21A). The intracellular organization and abundance of Wee1 remained the same after irradiation (figure 21C) and the addition of G2 checkpoint inhibitors. The only exception was with the addition of debromohymenialdisine, where there was an increase in nuclear signal intensity (figure 21E)

3.6f 14-3-3 β

The 14-3-3 family of proteins has been recently implicated to be involved in the subcellular localization of the phosphatases involved in the G2-M phase transition. The phosphorylation of cdc25 at Ser 216 mediates binding to 14-3-3 that contains a Nuclear Export Sequence (NES). The binding of cdc25 to 14-3-3 is believed to down regulate activity of cdc25 by sequestering it in the cytoplasm away from nuclear targets (Kumagai and Dunphy, 1999). Immunofluorescence studies show that in mock-irradiated cells, 14-3-3 was well distributed throughout the cytoplasm and nucleus, with the nuclear signal being noticeably stronger (figure 22A). Its intracellular distribution remained unchanged upon irradiation (figure 22C and E). There was no change after addition of debromohymenialdisine and UCN-01 (figure 22G and K) but after isogranulatimide treatment there was a decrease in nuclear signal intensity (figure 22I and K).

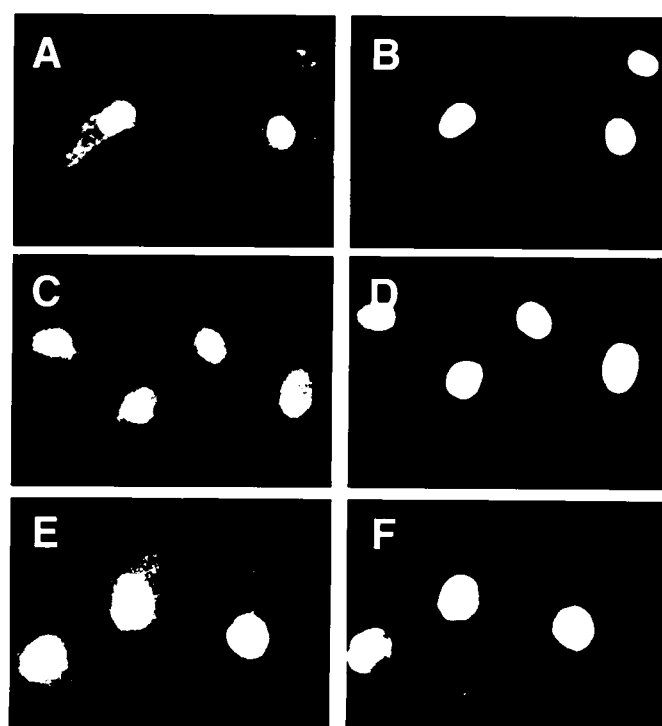


Figure 21. Nuclear/cytoplasmic distribution of Wee1

MCF-7 mp53 cells were mock irradiated (A, B), irradiated with 6.5 Gy and observed 19 hours later (C, D) or treated for three hours with 40 μ M debromohymenialdisine (E, F). Rows are matched photographs of cells showing Wee1 immunofluorescence to the left and DNA stain to the right.

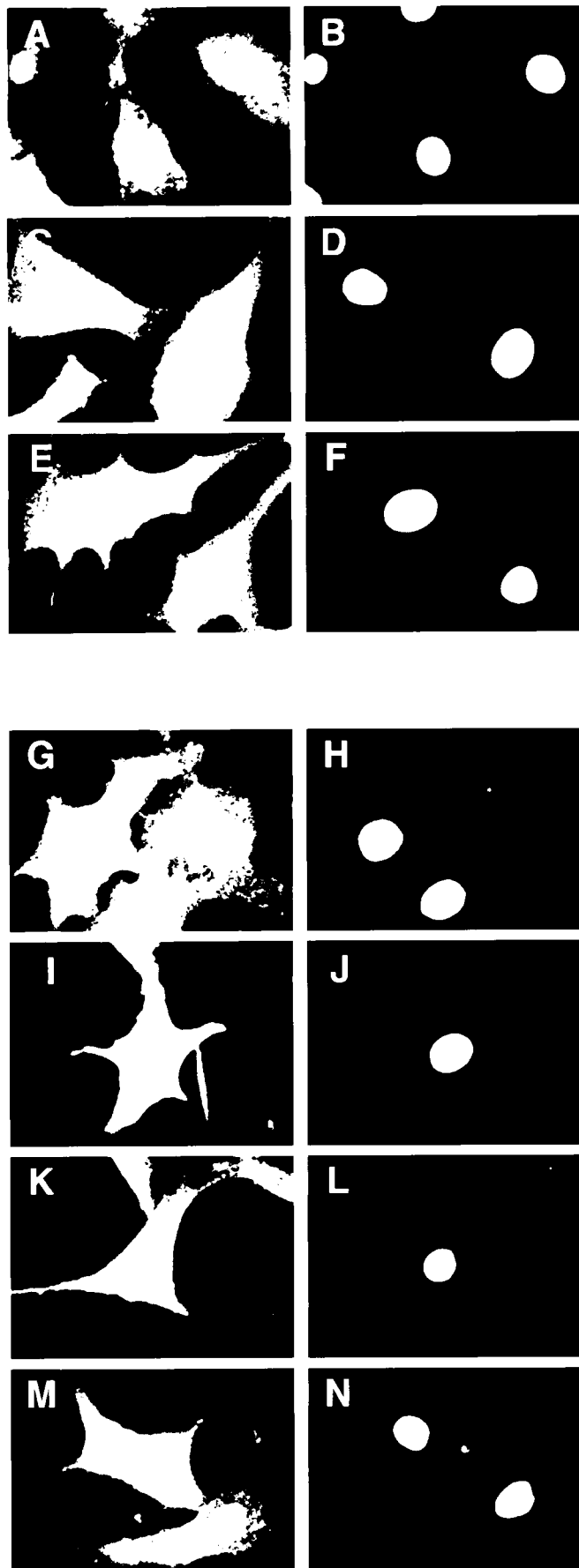


Figure 22. Nuclear/cytoplasmic distribution of 14-3-3

MCF-7 mp53 cells were mock irradiated (A, B), irradiated with 6.5 Gy and observed 16 hours (C, D) and 19 hours (E, F) later or 16 hours later treated for three hours with 40 μ M debromohymenialdisine (G, H), 10 μ M isogranulatimide (I, J), 10 nM UCN-01 (K, L) and 2mM caffeine (M, N). Rows are matched photographs of cells showing 14-3-3 immunofluorescence to the left and DNA stain to the right.

3.7 Debromohymenialdisine and isogranulatimide are in vitro inhibitors of GSK-3 β

The results of the immunofluorescence studies failed to elucidate the mechanisms by which debromohymenialdisine and isogranulatimide overcome G2 arrest. The structure of isogranulatimide is a rigid planar heterocycle (Roberge, 1998), a structural feature found in some protein kinase inhibitors, suggesting that isogranulatimide inhibits a protein kinase required for G2 arrest. To assess its ability to inhibit kinases, Kinetek Pharmaceuticals screened isogranulatimide against a panel of twelve common mammalian kinases: CDK1, CK-II, DNA-PK, ERK1, GSK-3 β , ILK1, LCK, MEK, PIM1, PKA, PAK, PKC, PKB and SRC. The results of the screen identified isogranulatimide as a strong inhibitor of GSK-3 β . To clarify this finding, debromohymenialdisine and isogranulatimide were assessed for their ability to inhibit this kinase.

Recombinant GSK-3 β protein with a GST tag was expressed in *E. coli* (strain BL-21) and purified using a glutathione-agarose column. Different concentrations of debromohymenialdisine and isogranulatimide were equilibrated with the recombinant GSK-3 β and reaction was initiated by the addition of a specific GSK-3 β peptide substrate along with [γ -³²P] ATP. The kinase activity was measured as pmol PO₄ incorporated/(nmol peptide x min) and plotted against the concentration of the drug (μ M) on a log scale (figure 23). The concentration at which half the kinase activity was inhibited (IC₅₀) was 0.03 μ M for debromohymenialdisine and 0.1 μ M for isogranulatimide. UCN-01 and caffeine were also assessed for their ability to inhibit the GSK-3 β kinase in vitro. UCN-01 exhibited no inhibition of kinase activity at its

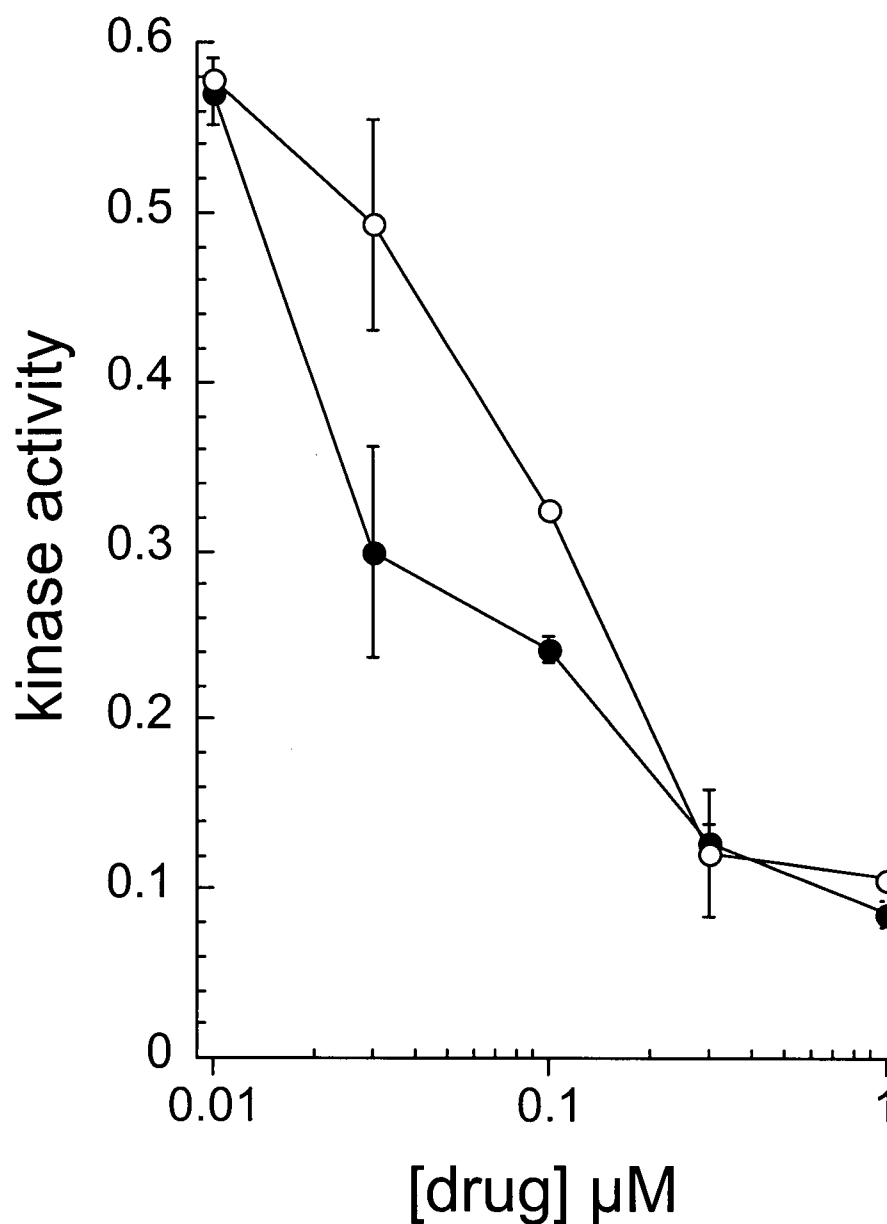


Figure 23. Debromohymenialdisine and isogranulatimide in-vitro inhibition of GSK-3 β kinase activity

Debromohymenialdisine (●) and isogranulatimide (○) were assessed for their ability to inhibit GSK-3 β kinase activity in vitro. Recombinant WT GSK-3 β was incubated with different concentrations of debromohymenialdisine and isogranulatimide at 30°C for 10 minutes. Then [γ - 32 P]ATP and GSK-3 β specific peptide substrate were added for 20 minutes at 30°C. The phosphorylation of the substrate peptide was determined as described in Materials and Methods. The kinase activity is expressed as pmol PO₄ incorporated/nmol peptide x min

optimum concentration of 100nM, whereas caffeine showed moderate inhibitory activity at 2mM.

3.8 Evidence for in-vivo inhibition of GSK-3 β by debromohymenialdisine and isogranulatimide

The preceding results show that debromohymenialdisine and isogranulatimide are potent inhibitors of GSK-3 β in vitro. Is this the case in vivo? GSK-3 β is a key component in the WNT/wingless signaling pathway that is involved in the regulation of β -catenin stability (Willert and Nusse, 1998); when activated, GSK-3 β enhances the degradation of β -catenin by phosphorylating a residue that targets β -catenin for degradation via the ubiquitin-proteosome pathway (Aberle *et al.*, 1997). Stimulation of this signaling pathway leads to the deactivation of GSK-3 β resulting in accumulation of β -catenin. As the intracellular amount of β -catenin increases, it translocates to the nucleus where it can mediate the expression of target genes. Thus, if debromohymenialdisine or isogranulatimide inhibited GSK-3 β in vivo, one would expect to see an increase in the intracellular amount of β -catenin.

3.8a Debromohymenialdisine and isogranulatimide causes an increase in nuclear abundance of β -catenin

To determine whether debromohymenialdisine and isogranulatimide can inhibit GSK-3 β in vivo, immunofluorescence studies were performed to visualize the intracellular organization and/or changes in abundance of β -catenin in response to the G2 checkpoint inhibitors. The results show that β -catenin was expressed in low amounts in both mock-irradiated interphase and irradiated cells as evidenced by the very faint

staining and was mostly in the nucleus (figure 24A, C and E). When cells arrested in G2 were treated with debromohymenialdisine, an increase in abundance of β -catenin was observed in the nucleus (figure 24G). Isogranulatimide also resulted in an increase in the nuclear intensity of β -catenin immunofluorescence (figure 24I) that was not seen with UCN-01 (figure 24M) or caffeine (figure 24N).

To confirm the observation by immunofluorescence that debromohymenialdisine caused an increase in nuclear β -catenin signal intensity, a β -catenin western blot was performed on nuclear extracts. MCF-7 mp53 cells were subjected to the same conditions as in the immunofluorescence studies. The cells were collected and nuclei were isolated and nuclear extracts prepared. Equal amounts of nuclear proteins, as determined by Coomassie Blue staining, were separated on a 10%SDS-PAGE and transferred onto a nitrocellulose membrane. A western blot was performed using anti β -catenin antibody.

The results clearly show that in interphase cells and in cells arrested in G2 at 16 or 19 hours after irradiation, there were low levels of β -catenin in the nuclei (figure 25). However, addition of DBH caused an increase in the nuclear level of β -catenin. Isogranulatimide caused a slight increase in nuclear β -catenin over interphase and irradiated cells. Caffeine and UCN-01 had no effect in abundance of β -catenin as compared to irradiated controls (figure 25). To summarize, the results of the immunofluorescence and western blots studies shows that the abundance of β -catenin increases in the nucleus. This provides strong evidence that debromohymenialdisine and possibly isogranulatimide are acting as *in vivo* inhibitors of GSK-3 β .

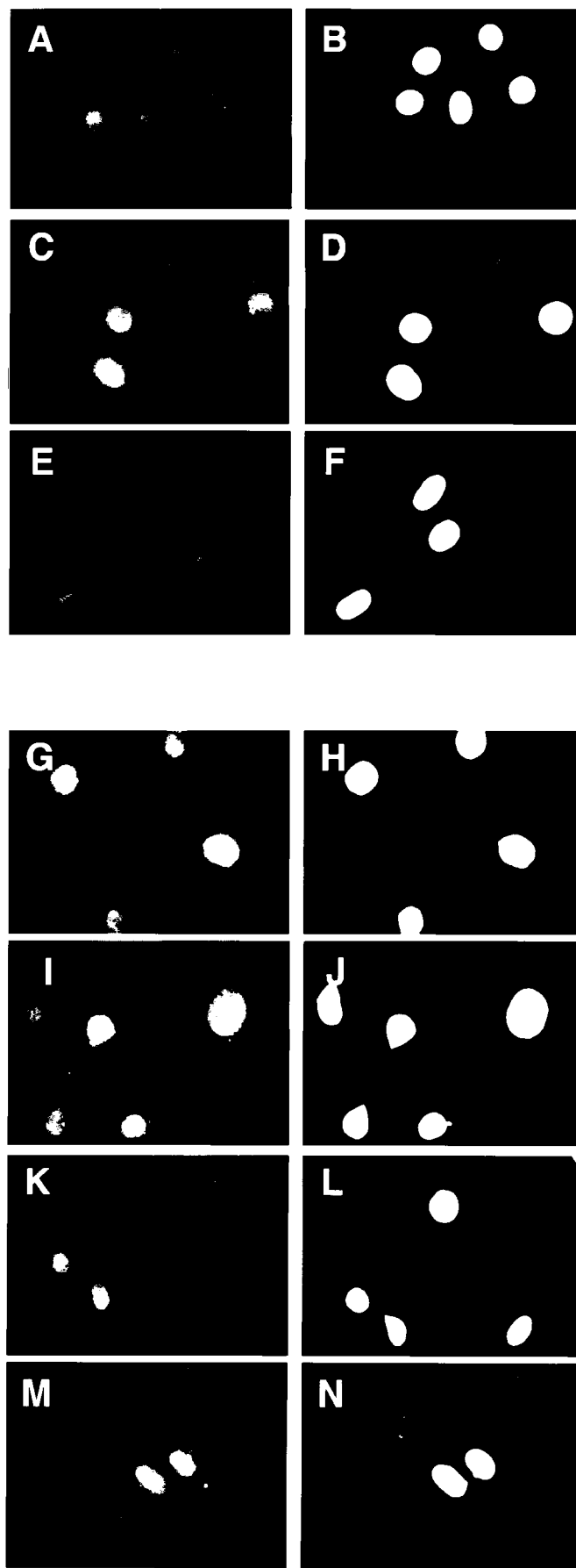


Figure 24. Nuclear/cytoplasmic distribution of β -catenin

MCF-7 mp53 cells were mock irradiated (A, B), irradiated with 6.5 Gy and observed 16 hours (C, D) and 19 hours (E, F) later or 16 hours later treated for three hours with 40 μ M debromohymenialdisine (G, H), 10 μ M isogranulatimide (I, J), 10 nM UCN-01 (K, L) and 2mM caffeine (M, N). Rows are matched photographs of cells showing β -catenin immunofluorescence to the left and DNA stain to the right.

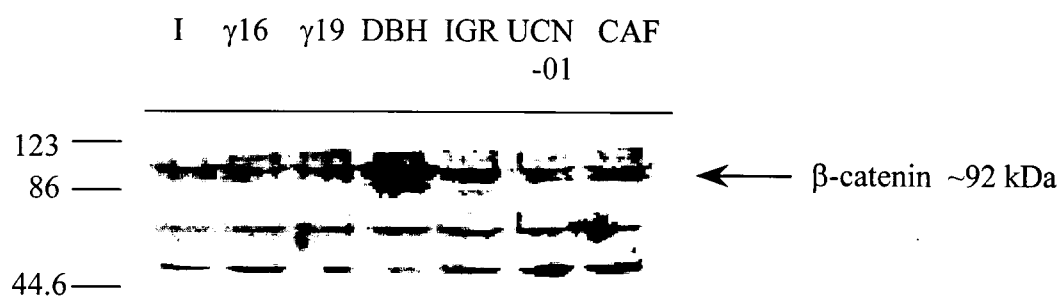


Figure 25. Nuclear localization of β -catenin in response to G2 checkpoint inhibitors

MCF-7 mp53 cells were irradiated and collected 16 hours later (γ 16) or 19 hours later (γ 19), or at 16 hours were incubated with debromohymenialdisine (DBH), isogranulatimide (IGR), UCN-01 or caffeine (CAF) for three hours. Unirradiated cells (I) were also collected. Nuclei were isolated, nuclear proteins resolved by SDS-PAGE and subjected to western blotting.

3.9 Effect of irradiation and checkpoint inhibitors on the subcellular localization of GSK-3 β

Immunofluorescence was performed to observe if there were any changes in the localization or abundance of GSK-3 β in response to irradiation or the addition of the G2 checkpoint inhibitors. In both cycling and irradiated cells, GSK-3 β was found mainly in the nucleus, with fine staining observed in the cytoplasm (figure 26A and C). Addition of debromohymenialdisine reduced the cytoplasmic staining but the nuclear signal remained strong (figure 26E). Isogranulatimide treatment (figure 26G) caused no change over the unirradiated or irradiated controls.

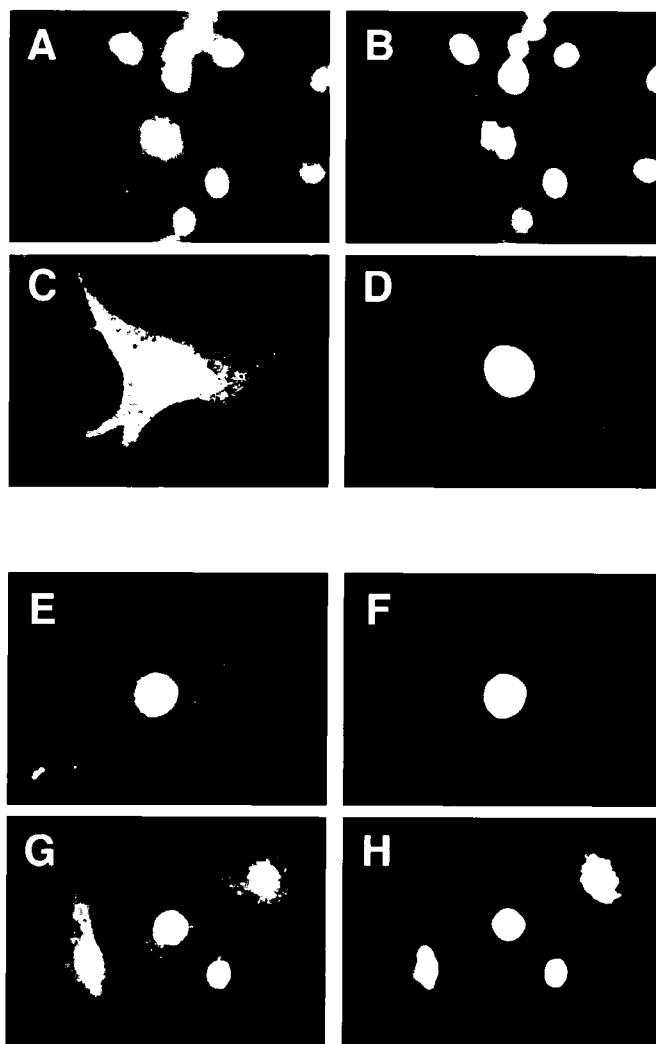


Figure 26. Nuclear/cytoplasmic distribution of GSK-3 β

MCF-7 mp53 cells were mock irradiated (A, B), irradiated with 6.5 Gy and observed 19 hours later (C, D) or 16 hours later treated for three hours with 40 μ M debromohymenialdisine (E, F) and 10 μ M isogranulatimide (G, H). Rows are matched photographs of cells showing GSK-3 β immunofluorescence to the left and DNA stain to the right

Chapter 4

Discussion

4.1 Identification of the novel G2 checkpoint inhibitors debromohymenialdisine and isogranulatimide

The known G2 checkpoint inhibitors include caffeine and its analogue pentoxifylline, staurosporine and its derivative UCN-01 (7-hydroxystaurosporine), and the protein phosphatase inhibitors fostriecin and okadaic acid (figure 7). Our initial screen of 1500 marine extracts resulted in the purification and isolation of four G2 checkpoint inhibitors. These included staurosporine and its oxazolidine derivative. The identification of staurosporine was important because it validated the effectiveness of the ELISA-based screen we used.

Two new G2 checkpoint inhibitors, debromohymenialdisine and isogranulatimide were isolated and their structures were elucidated in the Andersen laboratory. Debromohymenialdisine showed half-maximal activity at 10 μ M and maximal activity at 40 μ M. When MCF-7 mp53 cells arrested in G2 were treated with 40 μ M debromohymenialdisine for six hours, 45% of the cell population escaped G2 arrest which ranks the compound as a strong G2 checkpoint inhibitor. For comparison, 55% and 45% of MCF-7 mp53 cells escaped G2 arrest when treated with 2mM caffeine and 10nM UCN-01, respectively. DBH was found to potentiate death in irradiated MCF-7

mp53 cells over MCF-7 p53+ but also exhibited high toxicity towards unirradiated p53+ and mp53 MCF-7 cells suggesting it would not be a suitable agent for chemotherapy (unpublished results).

Isogranulatimide was active at lower concentrations ($IC_{50} = 2 \mu M$). Cells treated with $10 \mu M$ isogranulatimide showed a mitotic index of 35%, not as strong as debromohymenialdisine. Isogranulatimide alone showed mild cytotoxicity to MCF-7 cells with or without p53. However, treatment of irradiated MCF-7 mp53 cells with isogranulatimide potentiated killing in MCF-7 mp53 cells over MCF-7 p53+ cells when the DNA was damaged by ionizing irradiation. When MCF-7 cells were irradiated with 4 Gy and treated for 16 hours with $40 \mu M$ isogranulatimide, 90% of p53+ cells survived this treatment as compared to only 30% for mp53 cells (Roberge *et al.*, 1998). This makes isogranulatimide a good candidate for further investigation of its potential as a chemotherapeutic agent. Currently, analogues of isogranulatimide are being synthesized in the hopes of finding a more potent inhibitor of the G2 checkpoint pathway.

4.2 Debromohymenialdisine and isogranulatimide act upstream of Cdc2 and require the activation of a tyrosine phosphatase likely to be cdc25C.

The G2 checkpoint pathway in mammalian cells ultimately prevents the activation of the Cdc2 kinase. One mechanism is by inhibitory phosphorylation of Thr14 and Tyr15 of p34^{cdc2} by the kinases myt1 and wee1. The inactivation of Cdc2 causes the cells to arrest in G2, which is believed to enhance cell survival by allowing time for DNA repair to occur. In order for cells to enter mitosis, p34^{cdc2} must be dephosphorylated by the dual-specificity phosphatase, cdc25. However, mitosis can occur independently of Cdc2

as demonstrated in Gowdy et al (1998) who showed that FT210 cells, which have a temperature sensitive mutation in the $p34^{cdc2}$ gene, can enter mitosis when treated with okadaic acid or fostreicin at the non-permissive temperature.

I have undertaken studies to determine whether Cdc2 kinase activation occurred during the entry into mitosis induced by debromohymenialdisine and isogranulatimide. The results of histone H1 kinase assays showed that the activity of Cdc2 kinase in vivo was increased five-fold by both debromohymenialdisine and isogranulatimide. In addition, Cdc2 was dephosphorylated when treated with the G2 checkpoint inhibitors. Taken together the results show that debromohymenialdisine and isogranulatimide exert their intracellular effects upstream of Cdc2 causing the dephosphorylation and activation of Cdc2.

The G2 checkpoint inhibitors could activate Cdc2 in one of two ways. They could inhibit the weel or myt1 kinases responsible for inhibiting $p34^{cdc2}$ by phosphorylation at Thr14 or Tyr15 residues. Alternatively, they may cause the activation of cdc25C, which in turn would activate the Cdc2 kinase. To address this question, I have undertaken studies with the phosphatase inhibitor, phenylarsine oxide. Results show that PAO was able to antagonize G2 checkpoint inhibition by debromohymenialdisine and isogranulatimide. Since cdc25 is the only known tyrosine phosphatase that plays a role in the G2 checkpoint pathway, it is likely that debromohymenialdisine and isogranulatimide require the activation of cdc25 in order to induce entry into mitosis.

4.3 Identifying the in vivo targets of debromohymenialdisine and isogranulatimide

Efforts were undertaken to identify the *in vivo* targets of the novel checkpoint inhibitors by using a variety of approaches. Debromohymenialdisine was covalently bound via its primary amine group to epoxy-activated agarose with a spacer arm of 16 carbons. Cell extracts collected at various time points after irradiation were passed through both a DBH-agarose column and an agarose column. The bound fractions were examined for proteins that specifically interact with debromohymenialdisine but none was found. A plausible explanation is that the primary amine group of DBH used as the link to the epoxy-activated agarose is required for its specificity towards its target. If the primary amine is not exposed in the column then no protein binding will occur.

A different approach to try and identify *in vivo* targets of isogranulatimide was to radiolabel the compound and use it in a gel or in blot overlay assays. Isogranulatimide was found to react with iodine in the presence of trifluoroacetic acid. First, purified iodogranulatimide was tested for its effectiveness as a G2 checkpoint inhibitor. The activity was found to be somewhat diminished but experiments were continued. Extracts from irradiated MCF-7 mp53 were resolved by SDS PAGE and proteins were transferred onto a nitrocellulose membrane. Alternatively, the SDS PAGE gel itself was washed and the proteins were denatured and renatured. Overlay assays using ¹²⁵I-iodogranulatimide were performed on both the nitrocellulose and the SDS gel.

Exposure of the nitrocellulose membrane on film revealed very high background that could not be decreased even with extensive washings. It is believed that the high background was due to hydrophobic interactions of isogranulatimide with the nitrocellulose membrane. The assays performed using the gel gave much more promising results. The gel when exposed on film did reveal labeled protein bands.

However, all of the protein bands visualized corresponded to protein bands that were very abundant as determined by Coomassie blue stain. This suggests that the interactions of iodogranulatimide with proteins were of a non-specific nature.

Having failed to identify the direct *in vivo* target of debromohymenialdisine and isogranulatimide by these approaches, I then examined their effects as well as those of UCN-01 and caffeine on the abundance and subcellular localization of known cell cycle regulators using immunofluorescence. The cell cycle is regulated not only by modulation of the phosphorylation of proteins, but also by their abundance and intracellular location. For example, according to recent publications, *cdc25C* is actively sequestered in the cytoplasm away from its substrate *cdc2* during G2 arrest underscoring the importance of intracellular compartmentalization (Lopez-Girona, 1997).

Immunofluorescence studies were performed with a number of proteins that have been implicated either in the G2 checkpoint response, cell cycle control or in mitosis. These included cyclin A and cyclin B which form complexes with Cdk2 and Cdc2 respectively. Cyclin A/Cdk2 complexes are responsible for the transition through G1-S phase (reviewed in Reed, 1997; Dulic *et al.*, 1994) whereas cyclin B1/Cdc2 complexes are responsible for the transition into mitosis from G2 (Hoffmann *et al.*, 1993). In interphase cells, cyclin A was found to be mainly nuclear with fine cytoplasmic speckles whose abundance or localization remained unchanged in response to irradiation or addition of checkpoint inhibitors. Cyclin B1 in interphase cells was evenly dispersed throughout the cytoplasm with a noticeable accumulation in a ring around the nucleus. This suggests that cyclin B1 is being actively excluded from the nucleus. The subcellular organization remained the same when the cells were irradiated. However, after addition

of checkpoint inhibitors, in those cells that had entered prophase cyclin B1 was found to have a nuclear accumulation. Since nuclear accumulation of cyclin B1 is required for onset of mitosis (Jin *et al.*, 1998), the checkpoint inhibitors are inducing a normal entry into mitosis by acting upstream of Cdc2/Cyclin B1.

The cyclin-dependent kinases p33^{cdk2} and p34^{cdc2} were also examined. p33^{cdk2} was largely nuclear with very fine speckles in the cytoplasm which remained the same when the cells were irradiated or treated with the G2 checkpoint inhibitors. p34^{cdc2} on the other hand was very evenly dispersed throughout both the cytoplasm and the nucleus in interphase and irradiated cells. There was an increase in nuclear signal intensity of p34^{cdc2} when the cells were treated with debromohymenialdisine that was not observed with the addition of the remaining checkpoint inhibitors tested.

The CDK phosphatases, cdc25B and cdc25C, which play a role in the G2 to M phase by regulating the activation of the Cdc2 kinase were also included. In interphase cells, cdc25B was found to be mainly nuclear with fine cytoplasmic staining which was not altered with irradiation or addition of checkpoint inhibitors. Cdc25C in interphase cells was evenly dispersed in both the cytoplasm and the nucleus. However, localization of cdc25C was altered after irradiation as it became localized to a ring around the nucleus. When the checkpoint inhibitors were added to the irradiated cells, the localization of cdc25C was found to be similar to that before irradiation. The exception were cells treated with debromohymenialdisine which exhibited an increase in the nuclear signal intensity of cdc25C.

Wee1, the kinase responsible for inhibiting p34^{cdc2} by phosphorylation of its Tyr15 residue, was found to exhibit nuclear staining with fine cytoplasmic speckles. The

intracellular organization of Wee1 remained the same with irradiation or the addition of the G2 checkpoint. 14-3-3, a protein that is believed to mediate the activity of cdc25C towards its kinase substrate Cdc2 (Kumagai and Dunphy, 1999), was also included in these immunofluorescence studies. In interphase cells, 14-3-3 was found to be dispersed throughout the cytoplasm and the nucleus with the nuclear signal being noticeably stronger. The distribution remained unchanged with irradiation or the addition of the checkpoint inhibitors with the exception of isogranulatimide and caffeine which appear to cause a slight decrease in nuclear signal intensity.

To summarize the results of the immunofluorescence studies on known cell cycle regulators, irradiation does not cause a noticeable redistribution of these proteins with the exception of cdc25C. Addition of checkpoint inhibitors to irradiated cells does not cause any dramatic change in the intracellular distribution of cell cycle regulators other than those seen when the treated cells enter mitosis, which are the same as those seen in cells entering mitosis normally.

However, the immunofluorescence studies did provide some insight into the mechanism underlying Cdc2 kinase activation by the phosphatases cdc25B and cdc25C. Studies have shown that when cells enter mitosis, the Cdc2 kinase can activate cdc25C which can dephosphorylate and activate Cdc2 in an autocatalytic feedback mechanism (Hoffmann *et al*, 1993). It has been demonstrated that the cdc25B acts as a “starter phosphatase” dephosphorylating Cdc2 to initiate this autocatalytic loop (Lammer *et al.*, 1998). The immunofluorescence studies show that cdc25B is nuclear and that p34^{cdc2} and cdc25C are pancellular. Cyclin B1, which in G2 forms heterodimers with p34^{cdc2} (Jin *et al.*, 1998), was cytoplasmic with the exception of prophase cells where it was nuclear.

This result suggests that it is possible that cyclin B1/p34^{cdc2} is being kept inactive by its cytoplasmic localization away from the “starter phosphatase”, cdc25B rather than from cdc25C as literature suggests. When cells receive a signal to enter mitosis, cyclin B1/p34^{cdc2} is translocated to the nucleus where it is activated by cdc25B. This initial activation of Cdc2 then leads to the amplification of Cdc2 kinase activity through cdc25C.

4.4 Debromohymenialdisine and isogranulatimide are in vitro inhibitors of GSK-3 β

In vitro kinase inhibitor screens by Kinetek had indicated that isogranulatimide is a GSK-3 β inhibitor. I confirmed this result and showed that debromohymenialdisine is also a GSK-3 β inhibitor. Debromohymenialdisine and isogranulatimide inhibited the activity of the kinase with IC₅₀ values of 30nM and 100nM respectively. Caffeine and UCN-01 were also tested for their ability to inhibit the kinase at the concentrations at which they are G2 checkpoint inhibitors. It was found that caffeine at 2 mM inhibited 50% of the kinase activity and UCN-01 at 100 nM showed no inhibition. These data suggest that GSK-3 β could play a role in the G2 checkpoint pathway.

GSK-3 β is a major component of the WNT/wingless signaling pathway that is involved in the regulation of β -catenin stability (Reviewed in Willert and Nusse, 1998). When GSK-3 β is activated, it enhances the degradation of β -catenin by phosphorylating a residue that targets β -catenin for degradation via the ubiquitin-proteasome pathway (Aberle *et al.*, 1997; Hart *et al.*, 1998). Therefore, if the inhibitors were inhibiting GSK-3 β in vivo, one would expect to see an increase in abundance of β -catenin.

To confirm whether debromohymenialdisine and isogranulatimide are inhibiting GSK-3 β in vivo, immunofluorescence studies were performed with β -catenin. The results of the immunofluorescence showed that debromohymenialdisine and isogranulatimide caused changes in the abundance and intracellular compartmentalization of β -catenin. They caused an increase in immunofluorescence signal of β -catenin especially in the nucleus. These results were further supported by the western blots showing a strong increase in nuclear levels of β -catenin in cells treated with debromohymenialdisine and a slight increase in cells treated with isogranulatimide. It is important to note that neither caffeine nor UCN-01 caused an increase in β -catenin.

β -catenin is a 92-kD protein that serves a number of functions within the mammalian cell. It is associated with three cellular compartments, the plasma membrane, the cytoplasm and nucleus (Orsulic *et al.*, 1998). β -catenin binds directly to the intracellular domain of E-cadherin which binds to α -catenin, which connects the adherens junction complex with the actin cytoskeleton (Aberle *et al.*, 1994, Hulsken *et al.*, 1994, Jou *et al.*, 1995). In addition, β -catenin is also responsible for transducing the Wnt signals from the cell surface to the nucleus. In the nucleus, β -catenin complexes with members of the LEF/TCF family of DNA binding proteins where they can act as transcription factors upregulating Wnt responsive genes (Behrens *et al.*, 1996; Molenaar *et al.*, 1996).

Although GSK-3 β has not been linked to the G2 checkpoint or entry into mitosis, there is evidence that the GSK-3 β / β -catenin signaling pathway can control cell cycle progression. Mutations in the adenomatous polyposis coli (APC) gene that is implicated in the development of colon cancer result in the intracellular accumulation of β -catenin

(Munemitsu *et al.*, 1995). In addition, a mutant form of β -catenin that is resistant to degradation has been found in a wide variety of tumors including melanomas (Rubinfeld *et al.*, 1997), medulloblastomas (Zurawel *et al.*, 1998) and prostate cancer (Voeller *et al.*, 1998). The increase in β -catenin causes it to be translocated to the nucleus where it complexes with the LEF/TCF transcription factors to activate the expression of target genes. How the increase in LEF/TCF transactivation activity leads to the development of carcinomas remains to be determined. However it is quite plausible that upregulation of β -catenin leads to a deregulation of cell cycle control, because a number of cell-cycle genes have been identified whose promoter region contains the TCF/LEF binding site, including cyclin D1, cdc2, cdk2 and cdc25C (Tetsu and McCormick, 1999). Looking back on the immunofluorescence studies, it was observed that two of these cell cycle regulators, Cdc2 and cdc25C, increased in abundance in cells treated with debromohymenialdisine (figure 18G and figure 20G).

Taking these observations into account, I propose that DBH and possibly isogranulatimide are acting as *in vivo* inhibitors of GSK-3 β . The inhibition of GSK-3 β causes the intracellular increase in β -catenin that was observed in immunofluorescence and western blot studies. β -catenin translocates to the nucleus where it acts as a transcription factor complexed with the LEF/TCF family. The expression of genes that have yet to be identified causes the cells arrested in G2 to enter mitosis by a mechanism that is dependent on two key cell cycle regulators Cdc2 and cdc25C. Alternatively, GSK-3 β may have other downstream targets causing entry into mitosis by a signaling pathway independent of β -catenin.

4.5 Future directions

It is important to note that further studies are needed to determine whether the GSK-3 β / β -catenin signaling pathway is directly involved in the G2 checkpoint pathway or if in fact the activation of this pathway simply overrides G2 checkpoint control and causes entry in mitosis.

To answer this question, I propose that transfection experiments be carried out to create MCF-7 mp53 cell lines that can overexpress wildtype GSK-3 β , kinase-inactive GSK-3 β , β -catenin or indestructible β -catenin. Experiments would be carried out using these clones to determine what effect the overexpression of these proteins have on the cell's ability to arrest in G2 or to enter mitosis. In addition, any changes in GSK-3 β 's activity and its phosphorylation states should be examined in response to DNA damage. The data gleaned from such experiments may shed light on the role GSK-3 β may play in the G2 checkpoint pathway.

4.6 Conclusion

A screen of 1500 marine extracts for G2 checkpoint inhibitors using an ELISA-based assay has resulted in the purification and identification of four G2 checkpoint inhibitors. They include staurosporine and its oxazolidine derivative and two novel compounds, debromohymenialdisine and isogranulatimide.

I have determined that both debromohymenialdisine and isogranulatimide cause the activation and dephosphorylation of the Cdc2 kinase. Phenylarsine oxide, a tyrosine phosphatase inhibitor, was able to antagonize the ability of debromohymenialdisine and isogranulatimide to overcome G2 arrest. The results suggest that the inhibitors are acting

upstream of cdc25B or cdc25C that are responsible for the activation of cdc2 by dephosphorylation at the Thr14 and Tyr14 residues.

Affinity chromatography and gel overlay assays were used to try and identify the *in vivo* targets of debromohymenialdisine and isogranulatimide but proved unsuccessful. Immunofluorescence techniques were used to examine the abundance and localization of key cell cycle regulators in response to irradiation and addition of G2 checkpoint inhibitors but no dramatic changes were observed.

GSK-3 β was found to be potently inhibited by the G2 checkpoint inhibitors debromohymenialdisine and isogranulatimide with IC₅₀ values of 30 nM and 100 nM respectively using *in vitro* kinase assays. An increase in intracellular β -catenin was observed when cells were treated with debromohymenialdisine and isogranulatimide providing evidence that the inhibitors are inhibiting GSK-3 β .

References

- Aberle H. Bauer A. Stappert J. Kispert A. Kemler R. beta-catenin is a target for the ubiquitin-proteasome pathway. *EMBO Journal*. 16:3797-804, 1997
- Aberle H. Butz S. Stappert J. Weissig H. Kemler R. Hoschuetzky H. Assembly of the cadherin-catenin complex in vitro with recombinant proteins. *Journal of Cell Science*. 107:3655-63, 1994
- Akinaga S. Gomi K. Morimoto M. Tamaoki T. Okabe M. Antitumor activity of UCN-01, a selective inhibitor of protein kinase C, in murine and human tumor models. *Cancer Research*. 51:4888-92, 1991
- al-Khodairy F. Carr AM. DNA repair mutants defining G2 checkpoint pathways in *Schizosaccharomyces pombe*. *EMBO Journal*. 11:1343-50, 1992
- Anderson HJ. de Jong G. Vincent I. Roberge M. Flow cytometry of mitotic cells. *Experimental Cell Research*. 238:498-502, 1998
- Arnaud MJ. The pharmacology of caffeine. *Progress in Drug Research*. 31:273-313, 1987
- Banin S. Moyal L. Shieh S. Taya Y. Anderson CW. Chessa L. Smorodinsky NI. Prives C. Reiss Y. Shiloh Y. Ziv Y. Enhanced phosphorylation of p53 by ATM in response to DNA damage. *Science*. 281:1674-7, 1998
- Barinaga M. From bench top to bedside *Science*. 278:1036-9, 1997
- Behrens J. von Kries JP. Kuhl M. Bruhn L. Wedlich D. Grosschedl R. Birchmeier W. Functional interaction of beta-catenin with the transcription factor LEF-1. *Nature*. 382:638-42, 1996
- Berlinck RGS. Britton R. Piers E. Lim L. Roberge M. Da Rocha RM. Andersen RJ. Granulatimide and isogranulatimide, aromatic alkaloids with G2 checkpoint inhibition activity isolated from the Brazilian ascidian *Didemnum granulatum*: Structure elucidation and synthesis. *Journal of Organic Chemistry*. 63:9850-9856, 1998
- Bork P. Hofmann K. Bucher P. Neuwald AF. Altschul SF. Koonin EV. A superfamily of conserved domains in DNA damage-responsive cell cycle checkpoint proteins. *FASEB Journal*. 11:68-76, 1997

Chen P. Gatei M. O'Connell MJ. Khanna KK. Bugg SJ. Hogg A. Scott SP. Hobson K. Lavin MF. Chk1 complements the G2/M checkpoint defect and radiosensitivity of ataxia-telangiectasia cells. *Oncogene*. 18:249-56, 1999

Dalal SN. Schweitzer CM. Gan J. DeCaprio JA. Cytoplasmic localization of human cdc25C during interphase requires an intact 14-3-3 binding site. *Molecular & Cellular Biology*. 19:4465-79, 1999

Dulic V. Kaufmann WK. Wilson SJ. Tlsty TD. Lees E. Harper JW. Elledge SJ. Reed SI. p53-dependent inhibition of cyclin-dependent kinase activities in human fibroblasts during radiation-induced G1 arrest. *Cell*. 76:1013-23, 1994

Elledge SJ. Cell cycle checkpoints: preventing an identity crisis. *Science*. 274:1664-72, 1996

Fan S. Smith ML. Rivet DJ 2nd. Duba D. Zhan Q. Kohn KW. Fornace AJ Jr. O'Connor PM. Disruption of p53 function sensitizes breast cancer MCF-7 cells to cisplatin and pentoxifylline. *Cancer Research*. 55:1649-54, 1995

Fuse E. Tanii H. Takai K. Asanome K. Kurata N. Kobayashi H. Kuwabara T. Kobayashi S. Sugiyama Y. Altered pharmacokinetics of a novel anticancer drug, UCN-01, caused by specific high affinity binding to alpha1-acid glycoprotein in humans. *Cancer Research*. 59:1054-60, 1999

Gowdy PM. Anderson HJ. Roberge M. Entry into mitosis without Cdc2 kinase activation. *Journal of Cell Science*. 3: 3401-3410, 1998

Greenblatt MS. Bennett WP. Hollstein M. Harris CC. Mutations in the p53 tumor suppressor gene: clues to cancer etiology and molecular pathogenesis. *Cancer Research*. 54:4855-78, 1994

Guadagno TM. Newport JW. Cdk2 kinase is required for entry into mitosis as a positive regulator of Cdc2-cyclin B kinase activity. *Cell*. 84:73-82, 1996

Guo XW. Th'ng JP. Swank RA. Anderson HJ. Tudan C. Bradbury EM. Roberge M. Chromosome condensation induced by fostriecin does not require p34cdc2 kinase activity and histone H1 hyperphosphorylation, but is associated with enhanced histone H2A and H3 phosphorylation. *EMBO Journal*. 14:976-85, 1995

Hart MJ. de los Santos R. Albert IN. Rubinfeld B. Polakis P. Downregulation of beta-catenin by human Axin and its association with the APC tumor suppressor, beta-catenin and GSK3 beta. *Current Biology*. 8:573-81, 1998

Hatakeyama M. Brill JA. Fink GR. Weinberg RA. Collaboration of G1 cyclins in the functional inactivation of the retinoblastoma protein. *Genes & Development*. 8:1759-71, 1994

- Hatakeyama M. Weinberg RA. The role of RB in cell cycle control. *Progress in Cell Cycle Research*. 1:9-19, 1995
- Hirai H. Roussel MF. Kato JY. Ashmun RA. Sherr CJ. Novel INK4 proteins, p19 and p18, are specific inhibitors of the cyclin D-dependent kinases CDK4 and CDK6. *Molecular & Cellular Biology*. 15:2672-81, 1995
- Hoffmann I. Clarke PR. Marcote MJ. Karsenti E. Draetta G. Phosphorylation and activation of human cdc25-C by cdc2--cyclin B and its involvement in the self-amplification of MPF at mitosis. *EMBO Journal*. 12:53-63, 1993 Jan.
- Hulsken J. Birchmeier W. Behrens J. E-cadherin and APC compete for the interaction with beta-catenin and the cytoskeleton. *Journal of Cell Biology*. 127:2061-9, 1994
- Jin P. Hardy S. Morgan DO. Nuclear localization of cyclin B1 controls mitotic entry after DNA damage. *Journal of Cell Biology*. 14:875-85, 1998
- Jou TS. Stewart DB. Stappert J. Nelson WJ. Marrs JA. Genetic and biochemical dissection of protein linkages in the cadherin-catenin complex. *Proceedings of the National Academy of Sciences of the United States of America*. 92:5067-71, 1995
- Kaelin WG Jr. Recent insights into the functions of the retinoblastoma susceptibility gene product. *Cancer Investigation*. 15:243-54, 1997
- Kaufmann WK. Paules RS. DNA damage and cell cycle checkpoints. *FASEB Journal*. 10:238-47, 1996
- Kumagai A. Dunphy WG. Binding of 14-3-3 proteins and nuclear export control the intracellular localization of the mitotic inducer Cdc25. *Genes & Development*. 13:1067-72, 1999
- Lammer C. Wagerer S. Saffrich R. Mertens D. Ansorge W. Hoffmann I. The cdc25B phosphatase is essential for the G2/M phase transition in human cells. *Journal of Cell Science*. 111:2445-53, 1998
- Lavin MF. Shiloh Y. The genetic defect in ataxia-telangiectasia. *Annual Review of Immunology*. 15:177-202, 1997
- Levine AJ. p53, the cellular gatekeeper for growth and division. *Cell*. 88:323-31, 1997
- Liu F. Stanton JJ. Wu Z. Piwnicka-Worms H. The human Myt1 kinase preferentially phosphorylates Cdc2 on threonine 14 and localizes to the endoplasmic reticulum and Golgi complex. *Molecular & Cellular Biology*. 17:571-583, 1997

- Lopez-Girona A. Furnari B. Mondesert O. Russell P. Nuclear localization of Cdc25 is regulated by DNA damage and a 14-3-3 protein. *Nature*. 397:172-5, 1999
- McGowan CH. Russell P. Cell cycle regulation of human WEE1. *EMBO Journal*. 14:2166-2175, 1995
- McGowan CH. Russell P. Human Wee1 kinase inhibits cell division by phosphorylating p34cdc2 exclusively on Tyr15. *EMBO Journal*. 12:75-85, 1993
- Molenaar M. van de Wetering M. Oosterwegel M. Peterson-Maduro J. Godsave S. Korinek V. Roose J. Destree O. Clevers H. XTcf-3 transcription factor mediates beta-catenin-induced axis formation in *Xenopus* embryos. *Cell*. 86:391-9, 1996
- Mueller PR. Coleman TR. Kumagai A. Dunphy WG. Myt1: a membrane-associated inhibitory kinase that phosphorylates Cdc2 on both threonine-14 and tyrosine-15. *Science*. 270:86-90, 1995
- Munemitsu S. Albert I. Souza B. Rubinfeld B. Polakis P. Regulation of intracellular beta-catenin levels by the adenomatous polyposis coli (APC) tumor-suppressor protein. *Proceedings of the National Academy of Sciences of the United States of America*. 92:3046-50, 1995
- Nevins JR. E2F: a link between the Rb tumor suppressor protein and viral oncoproteins. *Science*. 258:424-9, 1992
- O'Connell MJ. Raleigh JM. Verkade HM. Nurse P. Chk1 is a wee1 kinase in the G2 DNA damage checkpoint inhibiting cdc2 by Y15 phosphorylation. *EMBO Journal*. 16:545-54, 1997
- Orsulic S. Huber O. Aberle H. Arnold S. Kemler R. E-cadherin binding prevents beta-catenin nuclear localization and beta-catenin/LEF-1-mediated transactivation. *Journal of Cell Science*. 112:1237-45, 1999
- Pagano M. Pepperkok R. Verde F. Ansorge W. Draetta G. Cyclin A is required at two points in the human cell cycle. *EMBO Journal*. 11:961-71, 1992
- Parker LL. Piwnicka-Worms H. Inactivation of the p34cdc2-cyclin B complex by the human WEE1 tyrosine kinase. *Science*. 257:1955-7, 1992
- Peng CY. Graves PR. Thoma RS. Wu Z. Shaw AS. Piwnicka-Worms H. Mitotic and G2 checkpoint control: regulation of 14-3-3 protein binding by phosphorylation of Cdc25C on serine-216. *Science*. 277:1501-5, 1997
- Pennisi E. Will a twist of viral fate lead to a new cancer treatment? *Science*. 274:342-3, 1996

Powell SN. DeFrank JS. Connell P. Eogan M. Preffer F. Dombkowski D. Tang W. Friend S. Differential sensitivity of p53(-) and p53(+) cells to caffeine-induced radiosensitization and override of G2 delay. *Cancer Research*. 55:1643-8, 1995

Rayl AJS. Oceans: Medicine chests of the future? *The Scientist*. 13:1-5, 1999

Reed SI. Control of the G1/S transition. *Cancer Surveys*. 29:7-23, 1997

Roberge M. Berlinck RG. Xu L. Anderson HJ. Lim LY. Curman D. Stringer CM. Friend SH. Davies P. Vincent I. Haggarty SJ. Kelly MT. Britton R. Piers E. Andersen RJ. High-throughput assay for G2 checkpoint inhibitors and identification of the structurally novel compound isogranulatimide. *Cancer Research*. 58:5701-6, 1998

Roberge M. Tudan C. Hung SM. Harder KW. Jirik FR. Anderson H. Antitumor drug fostriecin inhibits the mitotic entry checkpoint and protein phosphatases 1 and 2A. *Cancer Research*. 54:6115-21, 1994

Rowley R. Subramani S. Young PG. Checkpoint controls in *Schizosaccharomyces pombe*: rad1. *EMBO Journal*. 11:1335-42, 1992

Rubinfeld B. Robbins P. El-Gamil M. Albert I. Porfiri E. Polakis P. Stabilization of beta-catenin by genetic defects in melanoma cell lines. *Science*. 275:1790-2, 1997

Saka Y. Esashi F. Matsusaka T. Mochida S. Yanagida M. Damage and replication checkpoint control in fission yeast is ensured by interactions of Crb2, a protein with BRCT motif, with Cut5 and Chk1. *Genes & Development*. 11:3387-400, 1997

Sanchez Y. Wong C. Thoma RS. Richman R. Wu Z. Piwnicka-Worms H. Elledge SJ. Conservation of the Chk1 checkpoint pathway in mammals: linkage of DNA damage to Cdk regulation through Cdc25. *Science*. 277:1497-501, 1997

Savitsky K. Bar-Shira A. Gilad S. Rotman G. Ziv Y. Vanagaite L. Tagle DA. Smith S. Uziel T. Sfez S. et al. A single ataxia telangiectasia gene with a product similar to PI-3 kinase. *Science*. 268:1749-53, 1995

Sherr CJ. G1 phase progression: cycling on cue. *Cell*. 79:551-5, 1994

Sherr CJ. Mammalian G1 cyclins. *Cell*. 73:1059-65, 1993

Shiloh Y. Rotman G. Ataxia-telangiectasia and the ATM gene: linking neurodegeneration, immunodeficiency, and cancer to cell cycle checkpoints. *Journal of Clinical Immunology*. 16:254-60, 1996

Tam SW. Schlegel R. Staurosporine overrides checkpoints for mitotic onset in BHK cells. *Cell Growth & Differentiation*. 3:811-7, 1992

- Tetsu O. McCormick F. Beta-catenin regulates expression of cyclin D1 in colon carcinoma cells. *Nature*. 398:422-6, 1999
- Voeller HJ. Truica CI. Gelmann EP. Beta-catenin mutations in human prostate cancer. *Cancer Research*. 58:2520-3, 1998
- Wang Q. Fan S. Eastman A. Worland PJ. Sausville EA. O'Connor PM. UCN-01: a potent abrogator of G2 checkpoint function in cancer cells with disrupted p53. *Journal of the National Cancer Institute*. 88:956-65, 1996
- Waterman MJ. Stavridi ES. Waterman JL. Halazonetis TD. ATM-dependent activation of p53 involves dephosphorylation and association with 14-3-3 proteins. *Nature Genetics*. 19:175-8, 1998
- Weintraub SJ. Prater CA. Dean DC. Retinoblastoma protein switches the E2F site from positive to negative element. *Nature*. 358:259-61, 1992
- Willert K. Nusse R. Beta-catenin: a key mediator of Wnt signaling. [Review] [51 refs] *Current Opinion in Genetics & Development*. 8:95-102, 1998
- Xiong Y. Hannon GJ. Zhang H. Casso D. Kobayashi R. Beach D. p21 is a universal inhibitor of cyclin kinases. *Nature*. 366:701-4, 1993
- Zurawel RH. Chiappa SA. Allen C. Raffel C. Sporadic medulloblastomas contain oncogenic beta-catenin mutations. *Cancer Research*. 58:896-9, 1998